Fluvial terraces of the lower Mekong River reflect Quaternary global sea level fluctuations as a likely response to Himalayan glacial/deglacial runoff

Carling, P. A.¹, Meshkova, L.^{1,2}, Srivastava, A.³, Kinnaird, T.³, Ding, Z.⁵,

Robinson, R.4, Darby, S.E.1, Fan, X.5

5 6 7

1

2

3

4

¹School of Geography & Environmental Science, University of Southampton, Southampton, UK

²Current address: UK Head Office RSPB, The Lodge, Potton Road, Sandy, UK

8 9

³School of Earth and Environmental Sciences, The University of St Andrews, St. Andrews, UK

10 11 12

⁴Pittenweem, Fife, Scotland (formerly of the School of Earth and Environmental Sciences, The University of St Andrews), UK

13 14 15

⁵State Key Laboratory of Geohazard Prevention and Geoenvironment Protection, Chengdu University of Technology, Chengdu, China, 610059

17 18 19

20

22

23

24 25

26

27

28 29

30

31

32

33

34 35

36

37

38

39 40

41

42 43

16

*Corresponding author Xuanmei Fan: fanxuanmei 1@gmail.com

21 Abstract

Knowledge of the Quaternary history of the lower Mekong, the major river within Cambodia, is basic. Herein we advance understanding by investigations of river terrace topographic expression and stratigraphy. Satellite images, digital elevation models and fieldwork have been used to define the terrace elevations and extent. Three terrace levels can be recognised, separated in the vertical, lateral and temporal dimensions by distinctive sedimentary signatures. Strath surfaces and alluvial cover have been dated using terrestrial cosmogenic and optical luminescence protocols. The highest level (T1: notionally +100 m above present sea level) is a discontinuous, degraded, bedrock strath with a patchy veneer of well-weathered fluvial cobble gravel. T1 is younger than a regionally significant meteorite impact ~ 800 ka (Marine Isotope Stage¹ 20), and older than basalt flows on its surface (600 ka?). The T1 level was abandoned before 99.42 ± 7.52 ka (the end of the glacial MIS 5d), as the river incised in response to a rapidly falling sea level, to form a broad continuous strath terrace (level T2) exhibiting a thin alluvial cover, between 70 m and 40 m above sea level. The T2 terrace is composed of partially lateritic, interlayered, sand and gravel beds lying above weathered bedrock (blue/red clay). The basal deposits on the T2 level date to 70.65 ± 5.13 ka, following a sea level rise to a short-lived elevation of around +30 m around 80 ka (MIS 5a). The T2 level was progressively down cut between 57.73 ± 5.31 ka and 38.66 ± 2.40 ka (MIS 3). Steadily falling sea level sustained MIS 3 incision which reached c., 10 m above the modern river level c., 33.03 ± 3.09 ka, before the offshore minimum in sea level, c., 23 ka, i.e., towards the end of the Last Glacial Maximum. A loam-rich sandy terrace (T3; c., 0.45 ka (MIS 1)) is developed locally at c., +20 m above sea level. The timing of abrupt incisions, leading to the abandonment of the T1 and T2 levels, coincide with the onset of cool glacial stadials and falls in global sea level, whilst initial aggradation on the T2 level broadly can be associated with MIS 4. Despite a reduction in the contribution of glacial runoff from the Himalaya and Tibet towards the end of the Pleistocene, channel narrowing from T1 onwards has sustained the erosive power of the river, such that the rate of incision has only slowed within the Holocene.

¹ Marine Isotope Stage (MIS)

Key words: fluvial incision; strath terraces; glaciation; sea level change; Quaternary; Cambodia

44 45

Highlights

46 47 48

49

- Three main terrace levels along the Mekong River in Cambodia
- The two highest strath terraces have distinctive alluvial covers, whilst the lowest terrace is alluvial
- Three main incision phases occurred in glacial stadials MIS5d, MIS 3 and MIS 1 with an aggradation phase in MIS 4
- Incision corresponds to falling relative sea levels, reaching the present river elevation after 33 ka
 - Channel narrowing sustained incision; the rate fell in the Holocene as glacial runoff declined

54 55

53

1. Introduction

56

58

59

60

61

62

63

64

65

66

67

68

69

70

71

72

73

57 1.1. Intention of the investigation

The headwaters of the Mekong River drain a portion of the south-eastern Tibetan Plateau as well as part of the eastern Himalayan mountain chain whilst the main river flows due south through SE Asia (Fig. 1) to the Gulf of Thailand (Carling, 2009). The evolution of the Mekong River, south of the border between China and Laos, is poorly known (Brookfield, 1998; Hennig et al., 2018; Cao et al., 2023). Significant accumulations of sediment in offshore basins adjacent to the modern Mekong delta have been used to argue that the lower course of the Mekong has been in place since the late Eocene (Sladen, 1994; 2012; Métivier et al., 1999; Nie et al., 2018). Subsequent evolution, in part, is represented by distinct fluvial terrace levels along the Mekong in Cambodia (Saurin, 1935; 1966; 1967) which are indicators of a punctuated incision history of the lower Mekong. As will be shown latterly, the incision occurs at the same time as Quaternary climatically-controlled changes in the volume of sediment-laden runoff through the last glaciation (Liu et al., 2009), as ice sheets in the Eastern Himalaya SyntaxisTibetan Plateau expanded and subsequently receded, reflected in changes in regional sea level. Relative sea level is driven by epeirogenetic adjustments in the elevation of the land surface as well as by variation in sea level as water was sequestered in the global ice sheets and latterly released (Nakada & Lambeck, 1989). During the Last Glacial Period (LGP: 70 – 30 ka; Owen et al., 2008; Owen, 2009; 2010; Rupper et al., 2009), base level for the Mekong fell to approximately -116 m below the present sea level (Grant et al., 2014); sea level at that time being located up to 800 km from the modern coast (Hanebuth et al., 2011).

Herein, we investigate the geological information contained in the terrace sequences to better understand the Quaternary incision history of the river in Cambodia. Fluvial terrace levels between the towns of Stung Treng and Kratié (Fig. 1) are identified by altitude, morphology and by the differences in deposited sediments on each level. The incision history is constrained primarily using terrestrial cosmogenic dating, supplemented by optically stimulated luminescence (OSL) dating. We then discuss the relationship of the terrace levels to changes in glacial runoff and adjustments in sea level; the latter two changes defined from the literature.



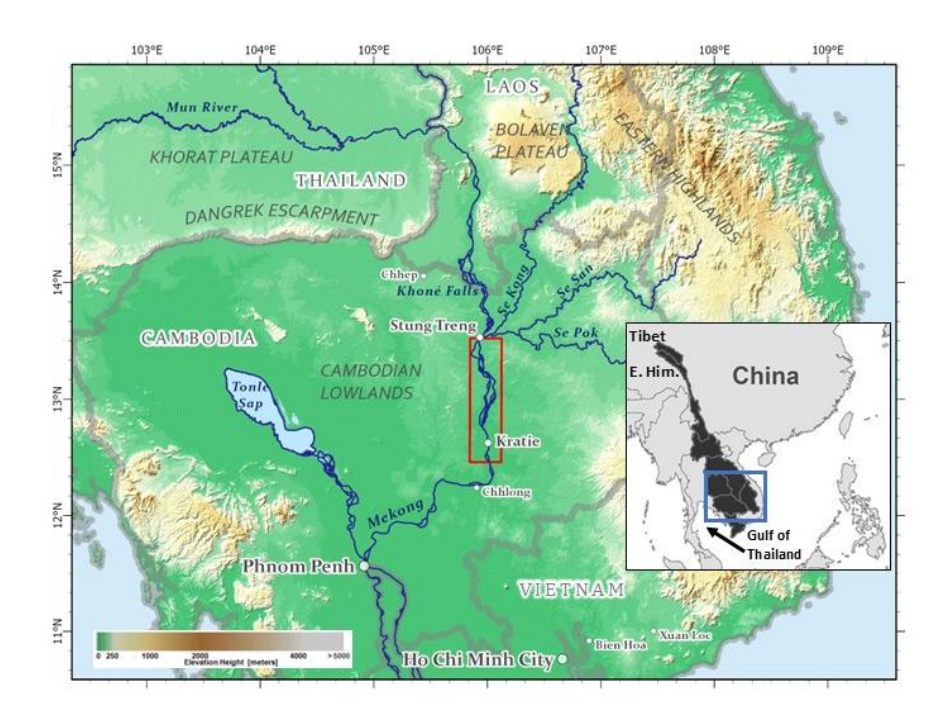


Figure 1: Location of the study region (blue box) within the broader area of SE Asia. The red box between the towns of Stung Treng and Kratié defines the study area. The inset shows the catchment area (black shading) of the Mekong River, with the headwaters in eastern Tibet and the eastern Himalayan mountains (E. Him.). National borders are shown as grey lines.

1.2. Regional geological setting

Mapping of the geology and geomorphological units in Cambodia by different agencies produce remarkably different results (Fig. 2), so the geology bordering the Cambodian reach of the Mekong was described summarily by Carling (2009) and by Meshkova and Carling (2012) based on fieldwork, to which the reader is

directed for local details. As is explained below, Saurin (1935; 1966; 1967), identified several fluvial terrace levels in Cambodia. Neither the SNMGP (1973; Fig. 2A) nor the JICA (2003; Fig. 2B) geological surveys identified Saurin's terrace levels, but they do map ancient alluvium, pediments, eluvial and colluvial sands bordering the Mekong that constitute sediments lying above strath terrace levels cut into the basement rocks. JICA (2003) recognized only one narrow river terrace level immediately north of Kratié. Much of the terrain within the elevation range of Saurin's terrace levels is underlain by the well-weathered, and erodible, Early Cretaceous Grès Supérieurs Formation and the late Jurassic to the early Cretaceous Terrain Rouge sedimentary rocks: sandstones, conglomerates, marls, shales, and siltstones (Racey, 2009). Volcanic rocks along the course of the river are represented locally by andesites, diorites and tuffs, whilst granitic and granodioritic intrusions crop out sporadically as erosion-resistant residual hills protruding above the alluvial/colluvial cover of the land surface (Fig. 3).

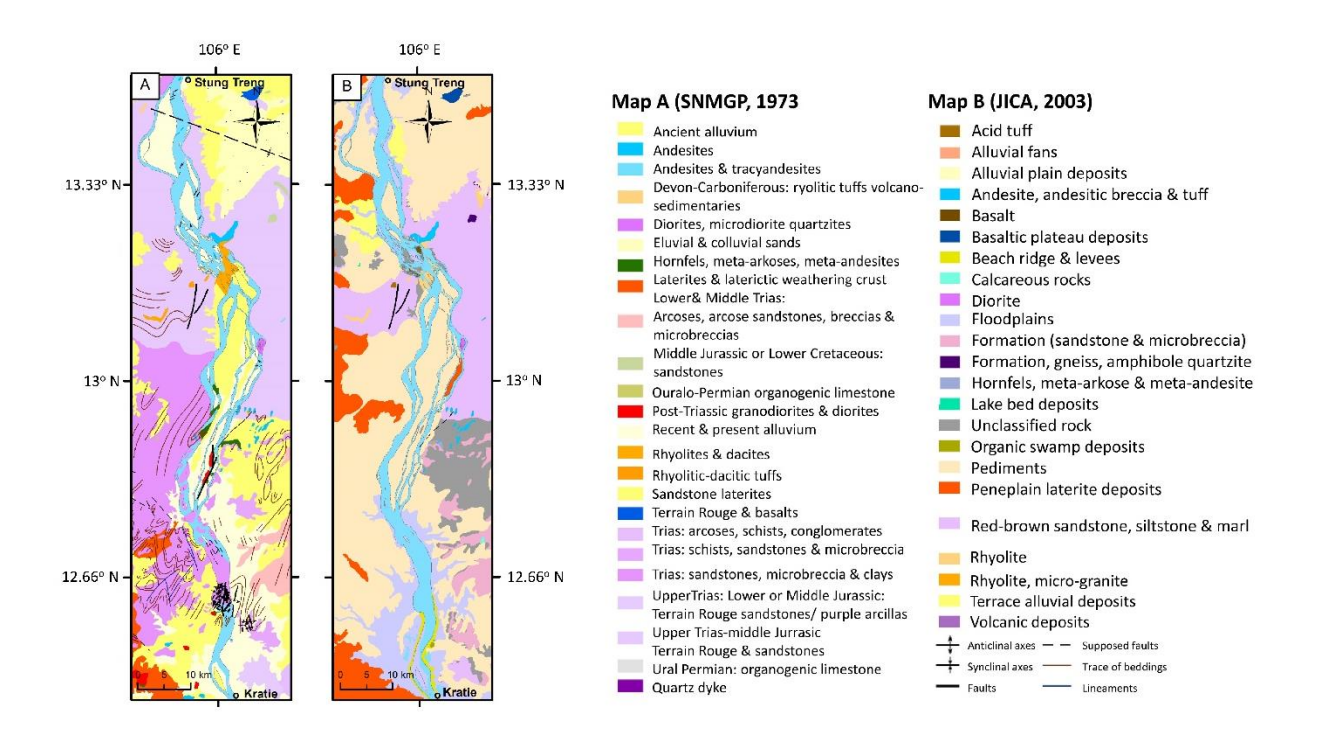


Figure 2: Geological maps of the study area (see text for details). Note that the rocks mapped by SNMGP (1973) as Triassic-Jurassic are now regarded as Late-Jurassic-Early-Cretaceous (Racey, 2009).

1.3. Epeirogenetic context

The lower Mekong flows south between the Eastern Highlands of central Vietnam to the immediate east and the Khorat Plateau to the immediate west (Fig. 1) and has followed its present course since at least the Mesozoic (Wang et al., 2020; Lai et al., 2023). So, to address the development of the Mekong in the Quaternary it is necessary to provide some context regarding the development of the river system during the Palaeogene/Neogene Periods. A substantial increase in terrestrial erosion has been related to the post-Miocene uplift of the Eastern Highlands and basalt eruptions (Lee & Watkins, 1998; Carter et al., 2000; Murray & Dorobek, 2004). Regional uplift may have been of the order of 600 m in the late Neogene (Bao & Hai, 1991; Hoang & Flower, 1998) at which time faulting in the region was active (Rangin et al., 1995) but subsequent faulting was insufficient to significantly affect the course of the Mekong River (Meshkova & Carling, 2012). Central Cambodia usually is regarded as relatively stable since 1 Ma (Saurin, 1967; Cung et al., 1998; Grant et al. 2014); although the Eastern Highlands, in places, are capped by basalts of Neogene and Quaternary age (Rangin et al., 1995; Hoang & Flower, 1998) associated with reducing regional uplift (Flower et al., 1992; Lee & Watkins, 1998). With the onset of global glaciation in the Quaternary, changes in eustatic sea level were relatively rapid in contrast to any terrestrial epeirogenic movements (Grant et al., 2014). Overall, as well as Quaternary sea level altitudes close to the modern sea level, there was a series of relative sea level falls, with the sediment from the Mekong accumulating as a lowstand Mekong delta (Matthews et al., 1997; Lee et al., 2001) within regionally subsiding basins offshore of the southern Vietnam coast. To summarize, structural terrain development of the river reach between Stung Treng and Kratié had ceased by the late Mesozoic. Within this reach of the river, Neogene and Quaternary deposits were formed in continental conditions under the influence of weathering and fluvial processes and, in the main, are not deformed by tectonism. So, for the purposes of interpretating controls on river terrace formation, Quaternary regional uplift or subsidence can be regarded as negligible.

1.4. Quaternary lateral stability of the Mekong River

108

109

110

111

112

113

114

115

116

117

118

119

120

121

122

123

124

125

126

127

128

129

130

131

132

133

134

To the west of the Mekong, using seismic data, Löffler *et al.*, (1984) reported significant incision of the Lower Mun River (Fig. 1) and two of its tributaries on the Khorat Plateau, close to the confluence with the Mekong. They recorded a buried palaeovalley below the modern Mun River that is 14km wide and 135m deep, incised 35m below present sea level and 130m below a sandstone cill near the confluence. Immediately to the north is

a further buried channel, 7km wide and 124m deep, which appears to be a 'cut-off' of the ancestral Mun River. These deep defiles are cut into Upper Cretaceous rocks and so can be presumed to be of Palaeogene origin. The upper 45m of the Mun basin fill is consistently dated as > 40,000 years BP using seven ¹⁴C assays (Löffler et al., 1984). The age and nature of the deeper fill is unknown but was determined by Löffler and colleagues from seismic data to be alluvial. Thus, the thick deposits reported by Löffler et al. (1984) are related to localized subsidence associated with the continued tilting eastwards of the Khorat plateau (Cooper, 2000) against the rising Eastern Highlands. The significance of these observations is that the sustained tilting of the Khorat Plateau to the east would ensure the Mekong flowed near its present course, east of the Khorat Plateau and west of the Bolavens Plateau, from at least the mid-Miocene as far as the Khoné Falls on the edge of the Dangrek escarpment (Fig. 1) and thence southwards to the ocean. Despite the pre-Quaternary uplift of the Khorat plateau, the north to south course of the Mekong from Stung Treng to Kratié has been stable during the Quaternary (Saurin, 1967; Cung et al., 1998; Grant et al. 2014). At Chhlong (Fig. 1) the river flows abruptly westwards following a W-E-aligned fault and, southwards, the highest river terrace has been subject to localized neotectonic downthrow of around 80 m (Carbonnel et al., 1972), whereas displacements of the highest terrace level have not been recorded to the north. The Palaeogene to Neogene Periods for the Khorat Plateau, taken together, represent an erosive period caused by tectonic uplift and inversion (Carter & Moss, 1999; Cooper, 2000; Clift et al., 2004) such that river sediments for this period are sequestered only in limited areas – mostly in Cambodia (Clift et al., 2004). Quaternary sediments primarily are located around the Tonlé Sap and the vicinity of Phnom Penh (UN, 1993; Steinhuer et al., 1997), although Neogene-Quaternary sediment further to the north and close to the Mekong River is mapped as 'ancient alluvium' in Fig. 2A and, in part, includes the sediment cover of river terraces.

135

136

137

138

139

140

141

142

143

144

145

146

147

148

149

150

151

152

153

154

155

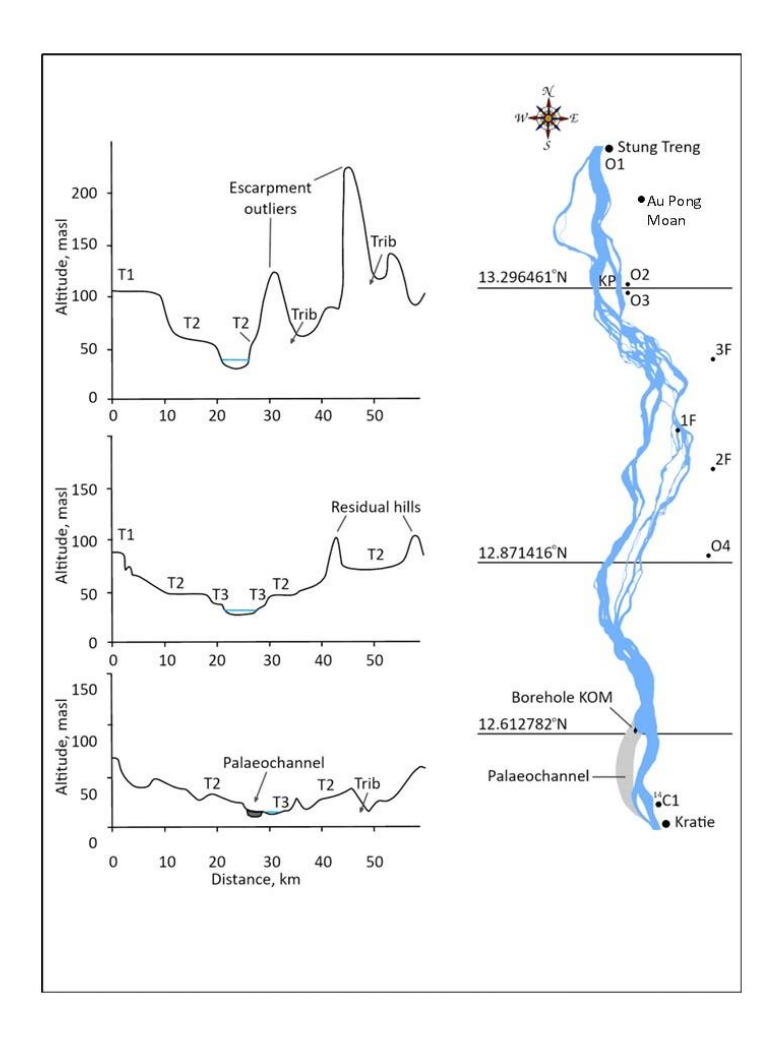


Figure 3: Three examples of cross-sections of the Mekong River and neighbouring terrain showing location of the terrace levels T1, T2 and T3, detailed in section 1.5. Escarpment outliers, residual hills and tributary (Trib) streams punctuate the cross-sections of terrace levels. Sample numbers refer to cosmogenic (1F-3F), OSL (O1-O4) and ¹⁴C samples (¹⁴C). (For details see Tables 1 and 2). KP is Kok Preah island.

1.5. The Mekong river terraces in Cambodia

In this section, the context of the terrace levels is described before detailing the methodology used in the current study to develop an improved understanding of terrace formation. The major river terraces reported by Saurin (1935; 1966; 1967) in Cambodia have not been traced northwards above the Khoné Falls into Laos/Thailand. The river above and below the Khoné Falls (within Thailand and Laos) is incised within bedrock with limited floodplain development (Wongsomsak, 1992; Carling, 2009) such that the present river corridor exhibits a stepped cross-section with an inner low-flow channel flanked by bedrock benches, *e.g.*, 8 m and 13 m above

river level (arl), in turn flanked by a higher elevation bench (c., 15 m arl) which is either cut into the alluvial bank line by high flows or represents a narrow accretionary terrace (Carling, 2009; Meshkova & Carling, 2012; their figs 6 and 11). Within Cambodia, as well as the 15 m level, distinct broad alluvial and strath terraces occur; the latter with thin alluvial cover occur above the river corridor either side of the river (Saurin, 1935; 1966; 1967), with nominal elevations above sea level (asl) of +100 m, +40-45 m, and +20-25 m (Takaya, 1967; Carbonnel, 1972).

Since Saurin (1935; 1966; 1967) proposed four terrace levels (inclusive of the 15 m level), there have been few subsequent investigations (Takaya, 1967; Carbonnel, 1972) and little clarity as to the ages, altitudes, and processes responsible for the sequence of terrace levels. Before 2000, when undegraded global positioning became available, field-surveyed altitudes along the Mekong reported in the literature were approximate elevations. Fieldwork for the present study showed that the altitude above present sea level of any given terrace increased from south to north in accord with the regional gradient of the Mekong, such that labelling spatially extensive terraces solely by elevation above the river or by altitude is ambiguous. As is explained below, the lowest of Saurin's levels is not regarded as a river terrace. Consequently, herein terrace levels are denoted as T1 to T3, from highest to lowest.

T1 level: The '+100 m terrace' of Carbonnel (1972). The T1 level is cut into a plateau that is often of similar altitude to T1 (Fig. 4). Carbonnel argued that the +100 m level was tectonically deformed, which is consistent with the suggestion of Nie *et al.*, (2018) that incision commenced in the Neogene related to late Miocene to late Pliocene regional subsidence in the vicinity of the southern Vietnam coast (Lee *et al.*, 2001). Saurin (1966) noted that the T1 terrace was severely degraded and difficult to define relative to the plateau surfaces that occur roughly at the same altitude. Degradation means that the gradient of the level is difficult to determine but the N-S slope ~ 1:4166, reported by Carbonnel (1972), is less than that of the modern river ~ 1:3585 between Stung Treng and Kratié, implying a base level to seaward of the modern coast. The T1 level occurs both to the west and to the east of the river and is cut into bedrock. A basalt flow occurs on the T1 surface at Xuan Loc, to the south of the study area, in southern Vietnam. Carbonnel & Pupeau (1969), using fission track dating, concluded that the last episode of major eruptive basalt flow at Xuan Loc occurred at 650 ka and Hoang & Flower (1998) redated the Xuan Loc basalt flow to between 830 ka and 440 ka. ⁴⁰K-³⁹Ar dates of around 600 ka +/- 200 ka for

the basalt flows above fluvial gravels in Thailand were believed to be the youngest Cenozoic basalts in the region (Sasada *et al.*, 1987). However, more recently, ⁴⁰K-³⁹Ar dates of between 790 and 51 ka have been obtained for basalt flows in the Bolaven volcanic field just to the north of the study area (Sieh *et al.*, 2020) so further dating of the basalt flows that lie on the T1 level would benefit from the application of more recent dating procedures. From the above, the T1 terrace level at Xuan Loc clearly pre-dates the basalt flows on its surface, although the level may not have been abandoned by the Mekong when the basalt flows were emplaced. A meteorite impact of regionally significant extent occurred *c.*, 800 ka (Sieh *et al.*, 2020; 2023). However, although tektites are found widely in Indochina, no *in situ* tektites have been reported from the T1 terrace level in Cambodia, which implies the terrace is younger than the impact event. These considerations sandwich the age of the initial cutting of the T1 level roughly to between 800 and 600 ka, *i.e.*, during the Mid Quaternary Period (Takaya, 1967).

T2 level: The '+40-45 m terrace' of Carbonnel (1972). The T2 level is continuous, laterally extensive, and can include altitudes up to c., 70 m asl, especially where colluvium has aggraded on the T2 surface below the escarpment on which the T1 level is developed (Fig. 4). Occurring both to the west and to the east of the river, throughout most of the study area the T2 level extends to the margin of the modern river corridor north of Kratié. Carbonnel (1972) reported the terrace slope as ~ 1:5000, indicating an offshore base level, in contrast to the modern river. Tektites found near Chhep, Cambodia and Bien Hoa, Vietnam, on the T2 terrace, were 40 Ar/ 40 K-dated to 600 ka (Saurin, 1966) which led Saurin (1966) and Carbonnel *et al.* (1972) to argue that the terrace predated the meteorite impact. However, the use of tektites found on the T2 surface for dating is unreliable, as the tektites were reported to be water worn and well-rounded (Saurin, 1966). Thus, the tektites were reworked and redeposited, and so likely not in stratigraphic context.

The following two levels occur intermittently along the course of the river and sometimes appear to grade into each other.

T3 level: The '+20-25 m terrace' of Saurin (1966) and Carbonnel (1972) was recorded to the south of Kratié, extending up to 1 km to the east from the eastern margin of the river corridor. In the present study, this level could not be traced northwards and, due to access difficulty, could not be traced with any reliability on the true

right bank of the river. The '+15 m terrace' of Carbonnel (1972); *i.e.*, the fourth and lowest level of Saurin (1967) is not regarded as a terrace level in this study, as is explained within the Results.







Fig. 4: A) View to the SE on the escarpment at an elevation of 128m (13.36052 N; 106.07857 E) showing the dissected plateau surface in the far distance; B) View to the S from the edge of the high level T1 terrace at an elevation of around 100 m. The T2 terrace is in the distance below the skyline.

2 Material and methods

2.1. Field survey and mapping procedure

Here, we identified the various terrace levels between Stung Treng in the north and Kratié in the south (Fig. 1) by altitude, morphology, and sedimentology. The terrace levels are dated using terrestrial ¹⁰Be cosmogenic surface exposure dating of bedrock outcrops, OSL dating of fluvial sediments on the terrace levels, as well as a single ¹⁴C radiocarbon-dated organic deposit. To further constrain the more recent incision history, the timing of abandonment of a substantial bedrock palaeochannel of the main river also was determined.

238

239

240

241

242

243

244

245

246

247

248

249

250

251

252

253

254

255

256

257

258

233

234

235

236

237

Examination of surfaces and sediment sections in the field, at around 50 localities (along the route 7 highway – not illustrated), chiefly between Kratié in the south and Stung Treng in the north, formed an important means to verify the nature of terrace levels. This transect was primarily along Saurin's (1966) +40-45 m (T2) terrace level. Excursions to the east were also made onto the T1 terrace level, and to the west to the T3 level and the low elevation bedrock islands and outcrops in the Mekong. Herein, only a brief report is given with respect to the sediment sections, sufficient to differentiate the various surface levels. Additional information is provided in Supplementary Information. Locations were recorded using a hand-held Garmin GPS and these coordinates were used to obtain altitudes in Google EarthTM and locations were mapped on a 50 m-resolution JICA ASTER digital elevation model (DEM). Given the planar nature of the terrain at each location the spatial errors (± 3 m) in the northing and eastings are insignificant. Errors in the determination of altitude were more difficult to define $(c_{\cdot,\pm} \pm 5 \text{ m})$ but this uncertainty still allowed to determine the typical altitudinal range of morphologically distinct terrace levels. Sedimentary sections were logged and photographed (Supplementary Information). Reclassification of the DEM using the slice function within ArcGIS 10, Spatial Analyst, allowed visualization of the elevation ranges in which the terrace levels might be sampled. The slicing procedure revealed elevation ranges across the study area that partly correspond to the altitudinal levels (100, 40 and 20 m asl) reported by Carbonnel (1972). An attempt to map terrace edges using SPOT 5 imagery and ground-truthing was abandoned as the terrace edges proved impossible to map accurately due to their large scale, physical degradation, and often subtle expression, coupled with the difficulty of physical access in remote and partially forested terrain. Nonetheless, a schematic cross-section details the relative altitudinal relationships of the terrace levels, the palaeochannel and the modern river (Fig. 5).

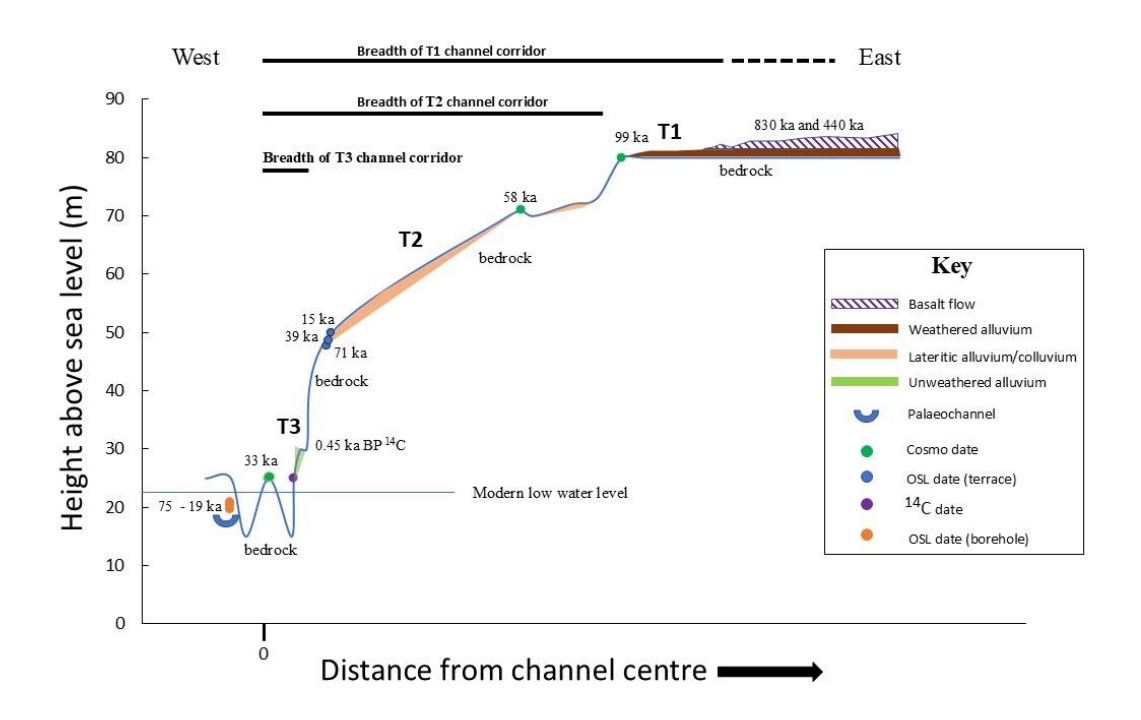


Figure 5: Schematic view of a stylized cross-section of the left bank of the Mekong looking upstream. Elevations are indicative and not absolute values. Terrestrial cosmogenic, luminescence and ¹⁴ C dates discriminate terrace levels (detailed within the Results section).

2.2. Be terrestrial exposure cosmogenic dating procedures.

Terrestrial cosmogenic radionuclides, such as ¹⁰Be, are produced and accumulate in minerals just a few metres into the land surface, due to exposure to secondary cosmic rays, and are lost due to erosion and radionuclide decay (Lal, 1991). To estimate the date when the modern river level was attained in relation to when the two main terrace levels, T1 and T2, were abandoned, we selected a bare rock outcrop in the middle of the Mekong, 6 m above the modern low-flow river level and two water-eroded bedrock prominences; one on the terrace level T2 and one on the outer edge of T1. Sampling from the top of bedrock prominences reduces the possibility of long-term alluvial cover shielding the now exposed surfaces, thus reducing nuclide production (Jones *et al.*, 2019). At each site, quartz-rich sandstone rock samples (0.5 kg) were obtained and the altitude, bearing, and tilt of the sampled surfaces were recorded. Sample No. 1F was obtained from the Mekong River near Ou Kreng (N: 13.08070; E: 106.05460; altitude *c.*, 28 m asl; Fig. S1A)) to represent the elevation of the modern river (low flow altitude *c.*, 22 m asl). Sample No. 2F was obtained from the T2 terrace level near Sre Kantang (N: 13.00727;

E: 106.15025; altitude *c.*, 70 m asl; Fig. S1B). Sample No. 3F was obtained from the outer edge of the T1 terrace just to the east of Phumi Prêk Preah (N: 13.177871; E: 106.172055; altitude *c.*, 80 m asl; Fig. S1C).

Sample preparation and isotopic measurements of the three samples were conducted at the Xi'an Accelerator Mass Spectrometry Center, Institute of Earth Environment, Chinese Academy of Sciences in Xi'an, China (see Supplementary Information). Our analytical approach entails three important assumptions concerning the nature of the cover of the strath surface (*e.g.*, Hurst *et al.*, 2016) that has been removed before the samples were collected. Prior cover consists of any bedrock that has been removed by fluvial abrasion during downcutting as well as the cover provided by alluvium on the strath surface. First, fluvial entrenchment into bedrock by at least 2 m, to form each terrace level, resulted in the ancient nuclide inventory within the rock overburden being removed. Second, the extended period related to the lateral cutting of each strath level was associated with a thickness of sediment accumulation sufficient to halt nuclide production in the surface of the abraded strath. Third, we assume that fluctuating river water levels and gravity were sufficient to remove sediment cover from each sampled prominence as the river abandoned each level. These assumptions mean that sampled surfaces began accumulating ¹⁰Be only from the time that the sediment cover was removed, such that the cosmogenic dates provide minimum ages for abandonment of each level. Due to the open aspect of each site, no topographic shielding corrections were necessary.

2.3. Luminescence and radiocarbon dating procedures.

OSL dating utilized the conventional multi-grain single quartz aliquot regenerative-dose (SAR) protocol (Murray & Wintle, 2000, 2003), with standard reliability checks. This procedure provides a means to date when minerals within sediment deposits were last exposed to sunlight (Rhodes, 2011). Deposition of fluvial sediment on the Mekong terraces will have occurred once downcutting to form each bedrock strath was replaced by a degree of alluviation. Thus, any OSL date will provide an age younger than that of the cut bedrock strath at the same location. The Mekong terrace levels are subject to surface wash and, being spatially extensive, they are crossed by minor tributaries and bioturbation is intensive throughout at least the first 1 m of depth within the soil and sediment profile. So, a range of ages for the sediments might be expected due to surface sediment

reworking and redeposition over time. In addition, colluvium overlies alluvium close to the inner edge of the T2 level, below the scarp of the T1 terrace. Alluvial/colluvial cover ranges from zero to c., 6 m thick, so basal alluvial sediment samples were preferred to provide the age when alluvium began to accumulate at any given locality. One sample was taken from the inner T2 margin and three samples constituting a single vertical profile were taken at the outer edge of the T2 level to assess the degree of biogenic reworking or the period of alluviation. Conventional techniques of dose rate estimation (Fig. S2) are suitable only for thick (>0.60 m) layers of alluvial sand (Kenworthy et al., 2014) so, in total, we obtained sand samples at seven discrete locations below 0.60 m depth and one sample at a shallow depth on the T2 level. In addition, one sandy matrix sample was taken from the basal gravels at the outer margin of the T1 level, but no *in-situ* dose rates were measured (e.g., Kenworthy et al., 2014), a point returned to within the Results section. Overall, four OSL samples from the centre of thick units of sand were taken from basal exposures close to the T2 strath surface. Steel tubes, 5 cm in diameter and 10 cm in length, were driven into exposures and then sealed with black plastic, providing around 200 cm³ of bulk sample. A single sample of wood (150 g) was obtained for ¹⁴C radiocarbon dating from the base of the outer margin of the T3 terrace level (analysis by Beta Analytic Inc.; see Supplementary Information). A petrol-driven percussion corer, equipped with a 0.5 m long core barrel (containing a sampling window), was used to retrieve a 5.5 m long core of the alluvial fill (borehole KOM; Fig. 1) within the un-named bedrock

used to retrieve a 5.5 m long core of the alluvial fill (borehole KOM; Fig. 1) within the un-named bedrock paleochannel (termed the KOM channel herein) just north of Kratié. The sampling was designed to constrain the timing of palaeochannel abandonment (Table 2) which should constrain the main channel incision history. Coring was terminated when the barrel encountered a thin indurated sand layer at 5.5 m depth immediately above bedrock. Four sand samples for OSL dating were taken from the core window at measured depths beneath the land surface (Fig. 5). The fifteen OSL samples were processed at the University of St. Andrews using standard procedures (see Supplementary Information).

3. Results

303

304

305

306

307

308

309

310

311

312

313

314

315

316

317

318

319

320

321

322

323

324

325

326

327

328

Variations in elevations across the study area revealed several elevation zones which correspond to the T1, T2 and T3 levels noted above but these could not be mapped precisely owing to the falling elevation of each terrace level from north to south and the difficulty in defining terrace margins as was noted in the Method section.

Nonetheless, the T1 terrace level is found typically between altitudes of 100 m to 80 m asl which is in accord with Carbonnel's (1972) notion of extensive dissection of this level. As noted in the Introduction, the T2 terrace level can include altitudes less than 40 m above the river towards the south and up to 60 m, or higher, towards the north and the east, especially where a colluvial cover derived from the scarp below the T1 level enhances the local elevation. Summary details of the alluvial cover on each terrace level are provided within Supplementary Information.

Above Stung Treng a distinct T1 outer terrace edge occurs at 103 m asl (13.49205° N; 106.0004° E) cut into a plateau that rises to around 113 m altitude at Au Pong Moan (13.437962° N; 106.076011° E) to the south. Although predominantly a strath, locally a cover of well-weathered, large, well-rounded cobble gravels occurs (*e.g.*, 12.899° N; 106.222833° E), up to 2.5 m thick, largely derived from reworking of local consolidated and lithified Triassic conglomerates (Fig. S4 and Supplementary Information). The cobble cover locally is laterized.

Below the T1 escarpment, Stung Treng town is constructed on the T2 strath terrace level, which here can range between 76 and 60m above the river level and extends 16 km up the Se San River at least to the river rapids at Nisay Sne Sesan (13.555122° N; 106.121902° E). The Mekong river islands, SW of Au Pong Moan, appear to be incised remnants of the T2 terrace level, having similar altitudes (Meshkova & Carling, 2012). The strath surface cuts across the basal lithological units and a distinctive blue or red clay at the base of the alluvial sections lies atop, and is derived from, the weathered basement rocks. The alluvial fill, forming the upper surface of the terrace, consists of a 1 m to 2 m thick cover of fluvial sands, with scattered well-rounded quartzite pebbles above a gravel bed, the latter frequently lateritic (Fig. S3-6 and Supplementary Information). Surface subaerial deflation of the sand bed has resulted in lag deposits of water-worn clasts on the surface of the terrace.

The T3 level is alluvial and discontinuous, occurring at altitudes mainly between 20 and 25 m asl. It primarily consists of loamy or silt/clay-rich alluvial sands with frequent pisolitic concretions (Fig. S8 and Supplementary Information), banked against the outer edge of the T2 strath. The alluvium overlies a blue-clay, which can be a

few metres-thick, which is the weathered basement as noted for the T2 level. The terrace sands are weathered, but less so than the T2 level sediments and can be overlain by a lag gravel due to surface deflation.

As was noted above, the '+15 m terrace' of Carbonnel (1972); *i.e.*, the fourth and lowest level of Saurin (1967) is not regarded as a terrace level in this study. This level, < 25 m asl consists of marginal banks of loose sand formed intermittently along the modern river by high river levels, no further than 10 km north of Kratié (see Fig. 2B). The normal annual maximum unregulated water level is around 10 m above the long-term low river level so the level can be inundated during exceptionally high river levels, as noted above, to elevations of c., 32 m asl. As such, it is not regarded as a terrace level in this study. Natural river levées only occur south from the Sambor Rapids, near Kratié.

3.2. ¹⁰Be terrestrial exposure cosmogenic ages

¹⁰Be apparent exposure ages are provided in Table 1. Given the low gradient of the T2 terrace level, the short distance between the upstream and downstream example river cross-sections (Fig. 3) and the uncertainty in GPS altitudes noted in the Method section, no adjustment is made in the altitudes of cosmogenic samples (and luminescence samples) when plotting these on an idealized cross-section of the true left bank of the Mekong River (Fig. 5). To interpret the incision history, we make use of the the LSDn ages which are more suitable for low-latitude regions than the St and Lm ages (Lifton *et al.*, 2014). Given that each sampled site may have previously had a thin alluvial cover the ages may be slight under-estimates. The bedrock within the outer edge of the T1 terrace level (c., 80 m asl) was exposed and therefore abandoned by the river no later than 99.42 \pm 7.52 ka. The T2 terrace level bedrock (c., 68 m asl) was exposed and abandoned after 57.74 \pm 5.31 ka. The outcrop in the modern river (c., 28 m asl) was reached some time prior to 33.03 \pm 3.09 ka, as frequent cosmogenic shielding due to inundation by river water during the annual high flows means the latter date is likely under-estimated. Exposure dating necessarily only yields a minimum limiting age of exposure yet, despite any uncertainty, the three ages are consistent with incision occurring within the Himalayan last glacial cycle (91 \pm 15 ka to 12.9 \pm 0.9 ka; Murari *et al.*, 2014; Owen & Dortch, 2014). The three ages young, as expected, from T1 through T2 to the modern outcrop. The extensive dissection of the T1 level (Carbonnel, 1972) may

indicate that abandonment occurred before or during MIS 6. However, taking a cautious approach to the interpretation of the exposure ages, if Carbonnel's assertion is correct that the T1 level was developed in the Mid Quaternary, then the date of 99.42 ka implies the T1 level was active throughout much of the Pleistocene Epoch, being abandoned only towards the end of the MIS 5d. Incision then was rapid, with a sufficient pause, commencing within the interglacial sub-stage (MIS-5a), to develop the T2 terrace level prior to 57.74 ka. Continued incision occurred throughout MIS 3, reaching the elevation of the top of the Ou Kreng outcrop (some 10 m or so above the modern bed level) towards the end of the sub-stage, and certainly before the end of the LGM. From this interpretation, the periods of strath development are relatively long in contrast to the apparent periods of rapid incision and abandonment of each level. A long period of stasis may have pertained on the T1 level, about which nothing is known.

392 3.2. Luminescence dates

382

383

384

385

386

387

388

389

390

391

393

394

395

396

397

398

399

400

401

402

403

404

405

406

407

408

OSL ages are summarized in Table 2 (see also Supplementary Information). The sandy matrix (sample O11, Table 2) recovered from within the cobble-gravel at the outer edge of the T1 level provided a date of $13.86 \pm$ 1.44 ka, which is not considered credible given the altitude (97 m) and the presence of a basalt flow (600 ka?) on the T1 surface. The considerable weathering of the cobbles here, in contrast to the slight weathering of the gravel on the T2 level, noted below, would indicate a great age for the T1 gravel. Rather, in-situ dose rates need to be measured at this T1 location to afford a reliable age determination (e.g., Kenworthy et al., 2014). The spatial variation in the small thickness of the alluvial cover on the T2 terrace means that the limited number of OSL dates available on the T2 level needs be considered with caution. Several samples (O3 to O10; Table 2) returned very young ages reflecting the widespread reworking of the surface deposits by small streams and surface wash after the level was abandoned. In addition, bioturbation by termites (in particular) and by tree fall is observed in some sections to at least the depth of 1 m. Of greater significance, the dates for two OSL samples (O1 and O2 which were obtained in the same vertical profile; Table 2), with the lowest sample close to the bedrock basement, are consistent with the ¹⁰Be dates. The T2 strath (c., 55 m altitude; sample O1; Table 2) was subject to aggradation of sediment at 70.65 ± 5.13 ka (i.e., around the beginning of MIS 4), following abandonment of the T1 level. The same location (sample O2; Table 2) was still subject to deposition of sediment at 38.66 ± 2.40 ka (Fig. 5), the difference in these two OSL dates, relative to the 10 Be date of 57.725 ka, reflects alluviation during progressive abandonment of this laterally inclined strath level throughout MIS 3 (Fig. 5). These two OSL dates essentially may bracket the development of the thin T2 alluvial cover more widely before surface reworking occurred; the latter is indicated by the 14.72 ± 0.95 ka age for a sample (O3), obtained closeby O2, but at a depth of 0.55 m (Fig. 5). The complex temporal and spatial response of the T2 sediment cover (potentially related to climatically driven periods of aggradation throughout MIS 3) is unclear without additional securely dated sediment sections. Nonetheless, the cosmogenic dating constrains the timing of incision phases. Abandonment of the T2 level at around 38 ka is consistent with the protracted sedimentation and subsequent abandonment of the (KOM) palaeochannel as the Mekong continued to entrench. The borehole KOM (Fig. 6A), through silt, reached gravel and compacted sand just above bedrock at 5.5 m depth (+19 m asl); which strata can be correlated with sand and gravel beds at 6 m and 9 m depth in borehole records 4102 and 4105 (Figs. 6B & 7), as reported by Stapledon et al. (1962). The mean ages for the two OSL samples in mid-core in borehole KOM are inverted but, considering the total uncertainty of the estimates, the ages of the two mid-core samples indicate deposition over essentially the same period of time (Table 2). Although all four luminescence dating samples are sandy, the clay content varied, such that variability in dosimetry may explain the inverted results (e.g., Kenworthy et al., 2014). Taken together, the three dates (75.42±5.72 ka to 43.21±3.11 ka) for the sandgravel basal deposits are interpreted to represent aggradation beneath flowing water within the KOM palaeochannel. The relatively early date for initial aggradation within the KOM palaeochannel implies that deep incision occurred near the modern main channel to form the KOM channel at the same time as T2 level was forming. This issue is returned to within the Discussion. The date of 19.43±1.96 ka coincides with a change from sand to silt deposition, consistent with deposition in a more quiescent backwater as the palaeochannel progressively was abandoned. This process occurred throughout the LGP. Thus, based on the ¹⁰Be assay for the rock outcrop at Ou Kreng, palaeochannel abandonment can be linked to the continued incision that occurred within the main river channel, with the modern river level being reached shortly after 33 ka. A conventional radiocarbon ¹⁴C age of 450 ±50 BP was obtained from wood buried at the base of the T3 terrace at a height above the modern river of ~ 10 m (Table 2). The calibrated age is CE 1600 to 1610 (cal BP 350 to

409

410

411

412

413

414

415

416

417

418

419

420

421

422

423

424

425

426

427

428

429

430

431

432

433

434

340) with 95% probability (Fig. S3). Given the recent age, it is evident that the deposit containing the wood is

due to high flooding levels at that time which inundated the land surface to +20 m above the low flow modern river level, depositing thick sand bars that contribute to the maintenance of the T3 level.



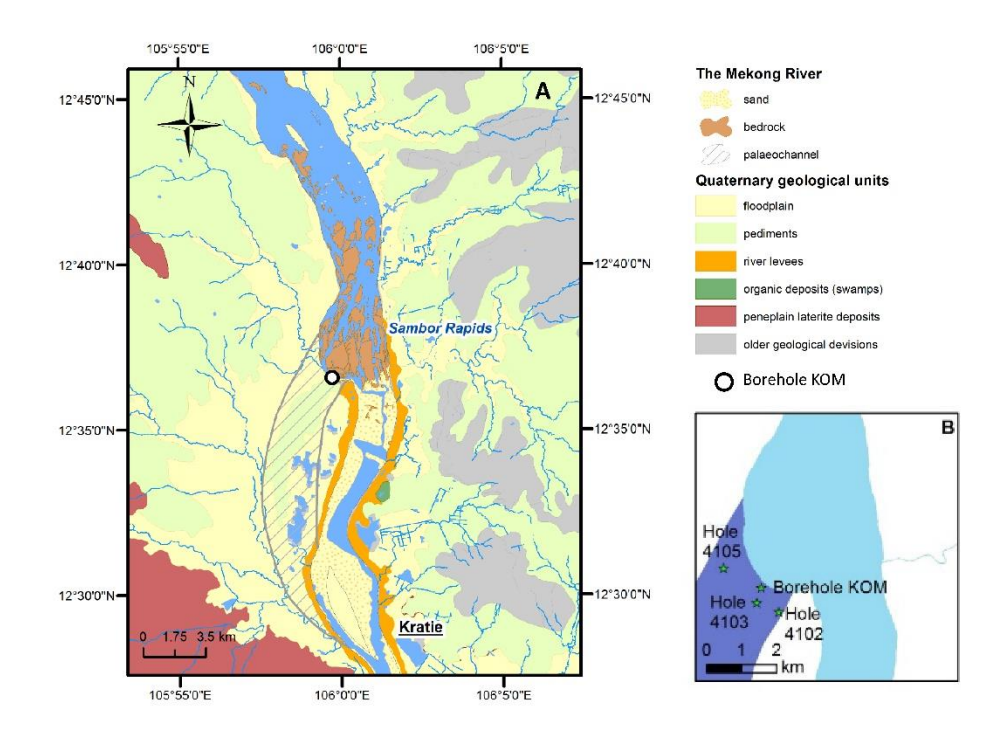


Figure 6: Location of palaeochannel borehole KOM. A) Relationship of the palaeochannel in relation to the local terrain and the modern river at the Sambor Rapids; B) Relationship of the borehole KOM to boreholes reported by Stapledon et al., 1962.

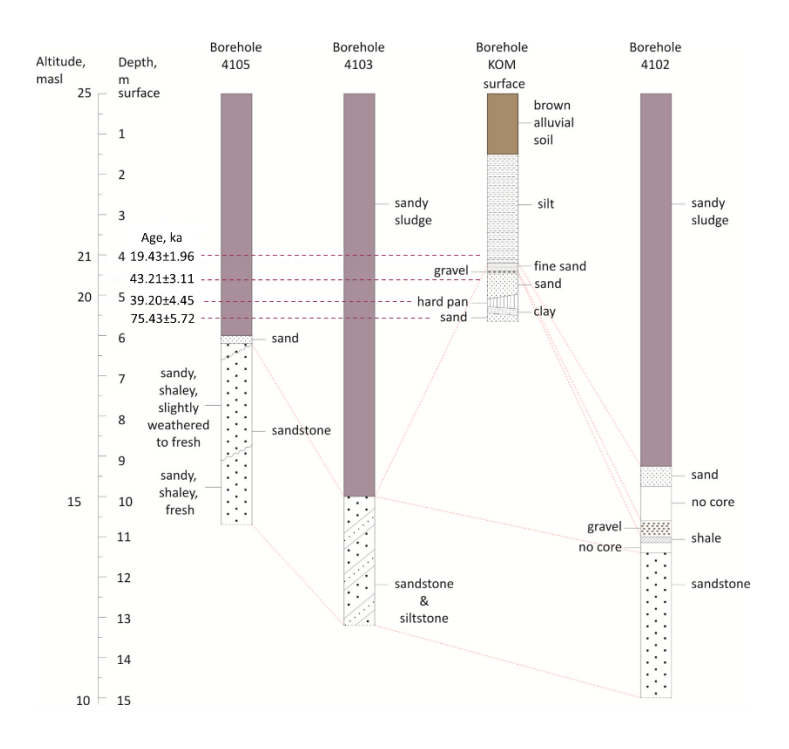


Figure 7: Borehole log for KOM (this study) compared to neighbouring borehole logs. Stratigraphic terminology for Boreholes 4102, 4103 and 4105 are as given by Stapledon et al. (1962).

4. Discussion

The three Cambodian terrace levels recognized in this study (T1, T2 and T3) accord with the '+100 m', '+40-45 m' and the '+20-25 m' notional altitudes of terrace levels reported by Saurin (1935; 1966; 1967) and (Carbonnel, 1972). It remains to be seen if these levels can be identified further north within Thailand and Laos, north of the Khoné Falls. The following text considers the incision history of the lower Mekong River related to relative sea level change, glaciation and deglaciation. Incision rates reported do not allow for any correction due to Quaternary rock uplift rates, which are believed to be negligible.

Bearing in mind there is quantified uncertainty in the ¹⁰Be dating, the observed average relative incision rate is 0.19 mm a⁻¹ from the outer edge of the T1 terrace level to the T2 terrace level based on the mean ¹⁰Be dates (uncertainty incision rate range: 0.28 mm to 0.15 mm a⁻¹). The average rate increases to 1.78 mm a⁻¹ (uncertainty range: 2.68 mm to 1.33 mm a⁻¹) for the observed incision from the T2 level to the top of the in-channel rock outcrop (which is 6m above the modern river low water level). As the top of the outcrop is ~ 10 m above the base of the modern channel there has been ~ 0.30 mm a⁻¹ of incision since 33 ka, which implies that incision

slowed during MIS 2 and during the early Holocene. During the Quaternary, the changes in the low latitude Indian monsoon and East Asian monsoon (Imbrie et al., 1992; Cheng et al., 2022; Hobart et al., 2023) and the Western Jet stream were associated with changes in precipitation (Pratte et al., 2024; Gao et al., 2024), consequent ice cover over the Himalaya and Tibetan Plateau (Barnett et al., 1989; Prell & Kutzbach, 1992) and related glacial runoff. Given the limited knowledge of the quantified links between Quaternary climate and glacial runoff in the region, sine qua non there is no scope to develop the detail of a connection herein, rather the focus is upon river incision and sea level changes with limited consideration of the likely implications for runoff. As is shown below, the relatively high rate of incision before MIS 2 can be related to progressively falling sea level, driven primarily by changes in Quaternary climate (e.g., Pan et al., 2003; Amos et al., 2007; Zondervan et al., 2022) and consequent increases in glacially-derived runoff (Grant et al., 2014) driving abrasion-incision due to an enhanced sediment load.

The increase in the rate of incision from the T1 level to the modern river outcrop might be explained by continued tectonic uplift but, as noted in section Epeirogenetic context, this is not tenable. The aggregational history of the T2 level clearly is not fully recorded within this study. Yet, if the observed sandy sediment cover on the T2 level (Figs. S5 to S7), dated to between MIS 4 and MIS 3, was of similar limited thickness during MIS 3 as today (0 to 6 m thick), the cover would not have impeded river incision into the bedrock. Rather, progressive incision from MIS 5d to MIS 2 has occurred with a concomitant narrowing of the Mekong's wetted channel breadth (Fig. 5), focussing erosive streampower. The styles of channel that existed on the broad T1 and T2 terrace levels are not known, but high yields of glaciofluvial sandy sediment during seasonal melt within glacial stadials, and a broad river corridor to disperse the discharge, would have favoured multiple braiding channels (Slingerland & Smith, 2004), cut into the thin sediment cover, enabling abrasive lateral planing of the rock strath surfaces to be sustained (Hancock & Anderson, 2002). As the Miocene weathered basement is readily eroded (Supplementary Information), a broad T2 strath surface developed. The inclination of the T2 surface towards the modern river (Fig. 5) clearly demonstrates that incision was steady and progressive from MIS 4 throughout MIS 3. As glaciofluvial runoff finally decreased during deglaciation (Smith et al., 1996), the braiding network would exhibit fewer channels, concentrating flow, leading to further incision (Germanoski & Schumm, 1993; Egozi & Ashmore, 2008). The deep incision of the KOM palaeochannel, contemporaneous with the early development of the T2 level, is not as surprising as it may first appear. The modern river, in the study reach, contains narrow bedrock troughs, reportedly 40 to 60 m deeper than the main channel bed (Carling, 2009), so the presence of the deep palaeochannel is not unusual. As a result of the significant narrowing late in MIS 3 (since 33.03 ± 3.09 ka) streampower became increasingly concentrated (at the same time as deglacial sediment flux was reducing), so cutting an anastomosed entrenched network of channels (Li et al., 2023) characterized by extensive exposed bedrock surfaces devoid of sediment cover (Turowski & Rickenmann, 2008; Inoue et al., 2014), much as seen today (Meshkova et al., 2013). The above interpretation is consistent with known regional glacial history. In the southern Himalaya, and within Tibet, ice cover was at its maximum pre-MIS 2 (Owen et al., 2002; Owen & Dortch, 2014), with significant ice cover throughout most relevant areas of the Himalayan syntaxis during MIS 3 (c., 75 to 30 ka) (Owen et al., 2008; Owen, 2009; 2010; Owen et al., 2009; Rupper et al., 2009). A marine δ^{18} O curve for the Indian Ocean (Leuschner & Sirocko, 2003) defines the alternating cooler and warmer periods in the climate within SE Asia for the last 140 ka, with key stages for Mekong incision from the T1 level indicated (Fig. 8A). As global climate change and a strong SW monsoon drives Himalayan glacial synchroneity (Finkel et al., 2003), so, early in the Last Glacial Period (MIS 4 – MIS 3), when the T2 terrace level was forming, the quantity of seasonal Himalayan-Tibetan melt water from the ice cover would have been sustained. The reduction in the incision rate during MIS 1 reflects a significant reduction in the fluid discharge and sediment load of the river as Himalayan-Tibetan glaciers retreated towards modern day ice cover (Grant et al., 2014). The relationship of the terrace

incisional history and glaci-eustatic sea level changes are considered next.

489

490

491

492

493

494

495

496

497

498

499

500

501

502

503

504

505

506

507

508

509

510

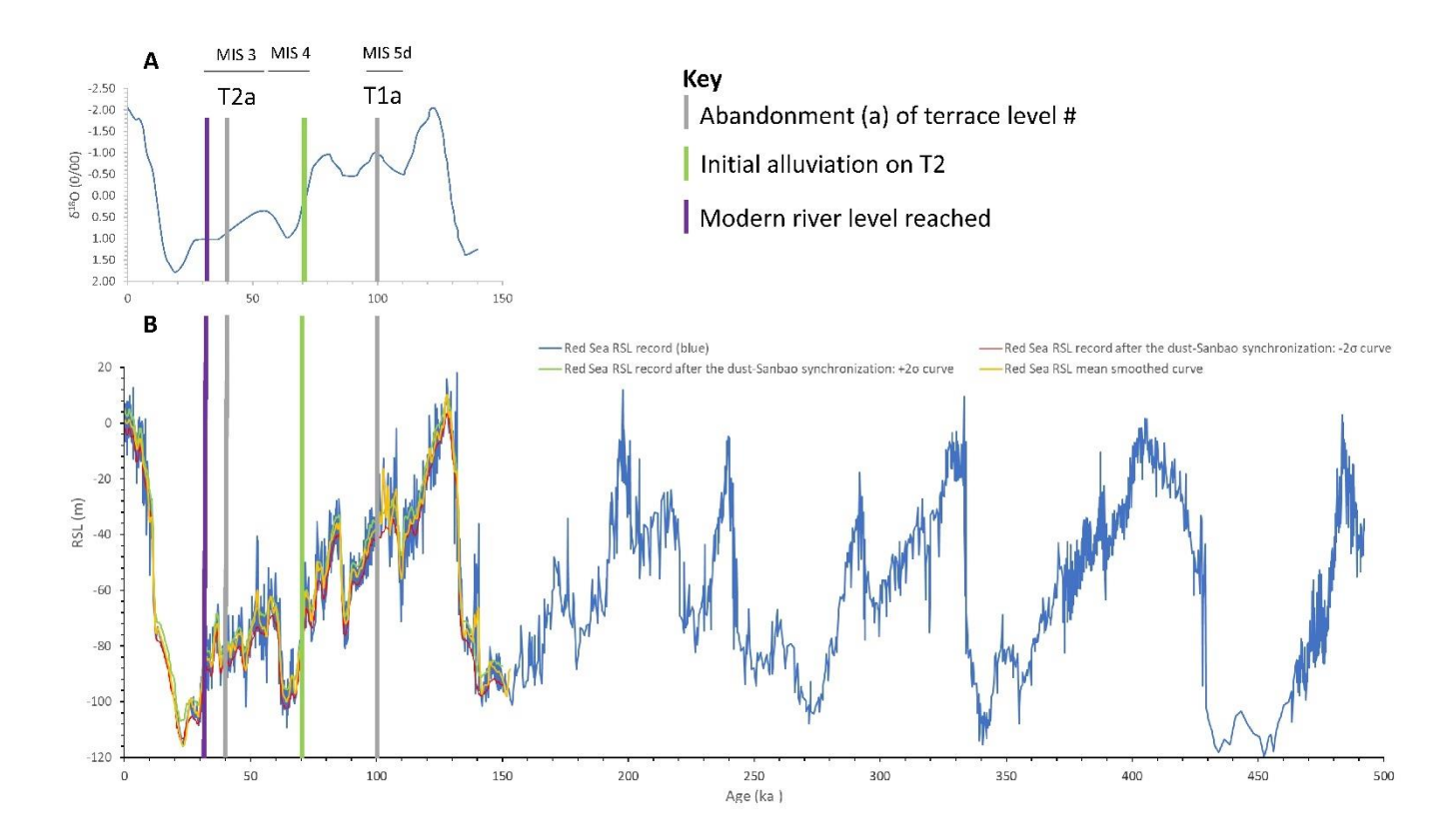


Figure 8: A) The Specmap stack marine oxygen isotope record (Leuschner & Sirocko, 2003); B) The Red Sea relative sea-level (RSL) over the last 500,000 years, based on tight synchronization to an Asian monsoon record (yellow curve: $\pm 2\sigma$ red and green curves); see Grant et al., 2014 for detail.

Although the T1 level may have been occupied by the Mekong River in the mid-Pleistocene, or earlier, there is limited firm evidence for the relationship of the terrace to sea level. However, Middle Pliocene global sea levels were around 25 m above modern sea level (Rohling *et al.*, 2009) which would accord with the relatively low gradient of the T1 level. More recently, during the last 1 M years, global sea level has oscillated, with sea level falling to around -100 m and similarly rising to \sim 0 m on several occasions (Rohling *et al.*, 2009; de Boer *et al.*, 2010; Hansen *et al.*, 2013). Towards the end of the Pleistocene, sea level on the Sunda Shelf and Vietnam Shelf was very low compared with the modern sea level, with the Sunda Shelf widely exposed during the MIS 3 (70 - 30 ka; Hathebuth *et al.*, 2000). Two independently derived relative sea level curves for global sea level adjustments since 150 ka, are essentially in agreement (Hanebuth *et al.*, 2011; Grant *et al.*, 2014). Global sea level *c.*, 135 ka was relatively high at *c.*, +0 m (Fig. 8B) and then it fell steady until 21 ka (Hanebuth *et al.*, 2009) although punctuated by three prominent rises that peaked *c.*, 110 ka, 80 ka and 50 ka with sea levels at *c.*, -20

m, -30 m and -60 m respectively (Fig. 8A) (Rohling *et al.*, 2009; Grant *et al.*, 2014) before falling sharply on each occasion. Following MIS 3, sea level rose rapidly from -116 m at 23 ka to -64 m by 13.1 ka (Hathebuth *et al.*, 2000; Tjallingii *et al.*, 2014). The bed level of the Mekong might be expected to respond to the three base level falls that followed the intermediate high stands (*c.*, 110 ka, 80 ka and 50 ka; Fig. 8B). These high stands tend to correlate with warmer intervals in the Pleistocene and the lower stands with cooler intervals of glacial stadials (NGRIP, 2004) such that the T1 and T2 incisional phases around 99 and 39 ka can reasonably be related with transitions to cooler climatic intervals. The relationship of the glacial stadials to sea level is considered next.

For the period of interest in the present study (*c.*, 100 ka to 14 ka) there is abundant evidence of significant glacial advances in the Himalaya (Owen *et al.*, 2008; Owen, 2009; 2010; Owen *et al.*, 2009) that may be linked broadly to regional sea level changes throughout MIS 5d to MIS 2. In the Eastern Himalaya Syntaxis-Tibetan Plateau, Quaternary glaciations responded in a complex spatial and temporal manner to the interplay of the South Asian Monsoon, East Asian Monsoon and the Westerly airstreams (Murari *et al.*, 2014) with glaciers advancing during periods of increased isolation (Owen *et al.*, 2014). However, the well-defined continuous sea level rise throughout the Holocene (MIS 1; Grant *et al.*, 2014) is related to rapidly diminishing global ice cover (Owen, 2009). Given the complexity of relationships prior to MIS 1, and the limited age constraints presented in this paper, it is not appropriate to attempt to close a correlation of the Mekong terrace development with variation in the Himalaya –Tibet glacial cycle. Nonetheless, some general summary observations may be appropriate.

The initial formation age of the T1 level is unknown but it is older than 600 ka as determined from the single 40 K- 39 Ar date (Sasada *et al.*, 1987). It is reasonable to attribute the deposition of large cobble-sized rounded clasts near the outer terrace margin to seasonal glaciofluvial runoff during the peak of the glacial sub-stage MIS 5d. On a more secure basis, the T1 level was abandoned at least by c., 99 ka, quite early in the last glacial cycle, preceding the time when Himalayan–Tibetan glaciers were advancing to maximum extent (Owen *et al.*, 2014; Murari *et al.*, 2014). However, the c., 700 ka between MIS 20 and MIS 5d includes at least four major drawdowns in sea level in the last 500 ka (Fig. 8B), and five corresponding pre-Last Glacial Period climatic stages (Murari *et al.*, 2014), for which there are no dated topographic surfaces indicating incision into the T1

level and no possibility of unambiguous correlation with glacial stadials, interglacials and changes in regional precipitation (Gao *et al.*, 2024). This situation is not unique, despite multiple glacial cycles, Pan *et al.*, (2003) recorded only five strath terraces over the past 900 ka for the Shagou River on the Tibetan Plateau. The conundrum of the lack of evidence for early incision to form the T1 level can be resolved if the Mekong cut down prior to MIS 5d to form a trough above that of the T2 level following which the bed level oscillated with alluviation and incision of the trough fill until fresh incision into the bedrock of the T1 margin occurred *c.*, 99 ka. The aggregational history of the T2 level can only be resolved with a more spatially dense pattern of OSL sampling, ideally from strategically located boreholes rather than the largely random locations of stratigraphic sequences (often incomplete) exposed in sandpits and stream sections.

555

556

557

558

559

560

561

562

563

564

565

566

567

568

569

570

571

572

573

574

575

576

577

578

579

580

581

Notwithstanding the uncertain early history, the T1 level was abandoned towards the end of MIS 5d during the transition to the interglacial substage MIS 5c. Thus, the T2 terrace level was initially cut into the bedrock prior to MIS 4 when aggradation occurred on the strath $c_{\cdot \cdot}$, 71 ka (MIS 4), but otherwise the T2 terrace largely developed as a strath throughout MIS 3, reflecting a persistent regional monsoon-influenced cool glacial climate at that time (Murari et al., 2024) and a persistent sea level below modern level (Bloom & Yonekura, 1990). The thin cover of T2 sediment allowed the braiding river to continue to down cut into the bedrock as the individual channels would have run over bedrock between alluvial banks such that the T2 level progressively fell from c., 70 m asl (e.g., lower-study-reach; Fig. 3; Table 2) to 41 m asl, following which the T2 level was abandoned. Progressive abandonment of this level may be reflected in the slope of the T2 level transverse to the river course (Fig. 5) and a reduction in the degree of laterization of the T2 sediments from the T2 margin distal from the river to the T2 margin close to the river (Takaya, 1967) which would reflect generally older sediment farther from the river. Nonetheless, the T2 level was abandoned at the transition to the cool stadial of MIS 2, when seasonal glacial meltwater became concentrated essentially within the modern river planform. Although the relative roles of key climatic drivers for changes in runoff are far from clear (Clark et al., 2012; Delgado et al., 2012; Cai et al., 2025), deglaciation from 19 ka would have increased runoff at the same time as the East Asian Summer Monsoon intensified leading to higher precipitation (Peterse et al., 2011). This scenario, of increased incision during deglacial periods, is consistent with the earlier view of Vozenin-Serra & Privé-Gill (1991) who (based on the taxonomy of sub-fossil wood found within T2 level) tentatively argued that the distal portion of the T2 level was pre-MIS 2 and that the T3 level was post-glacial. Furthermore, the incision history (reported herein) for the Lower Mekong is compatible with the incision history of the upper Mekong in the south-eastern part of the Tibetan Plateau, where incision or aggradation was related to glacial-interglacial climatic changes (Zhou *et al.*, 2024).

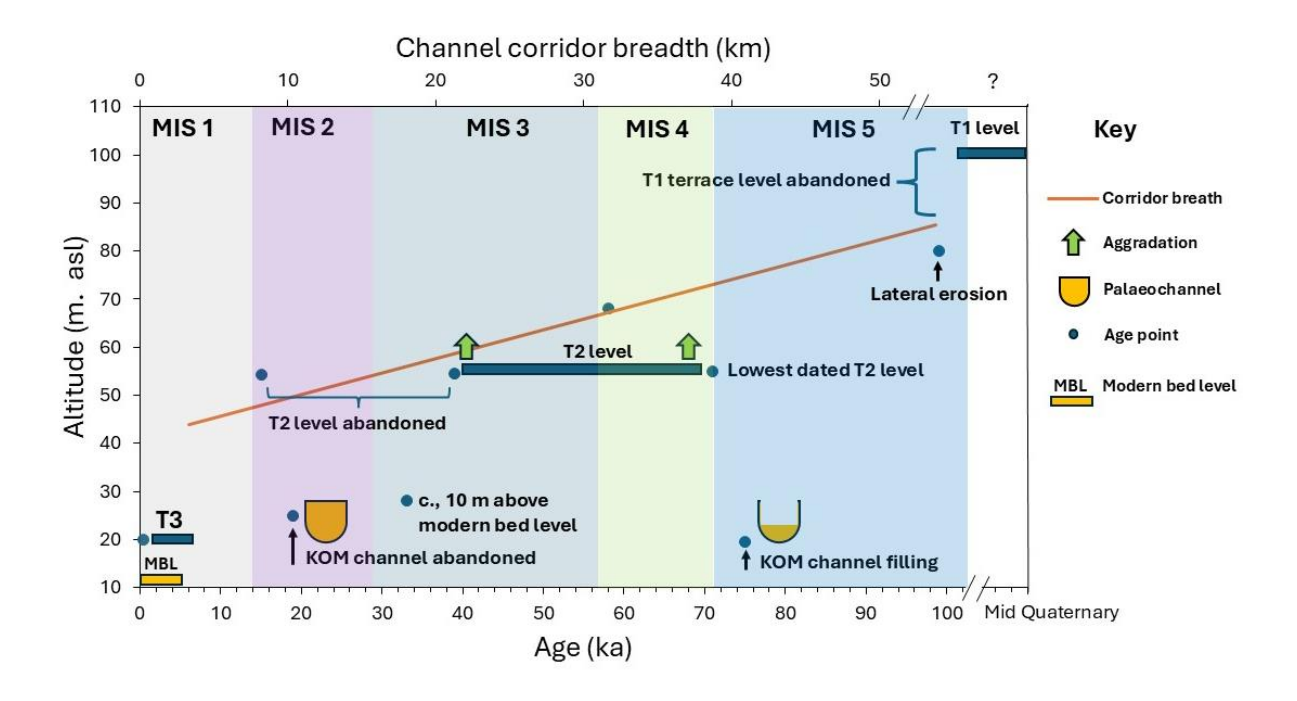


Figure 9: Schematic summary of the incision history of the Mekong River in Cambodia. Altitudes are indicative, as there is some variability in the elevation of the terrace levels. Age points include terrestrial cosmogenic, luminescence and ¹⁴ C dates (detailed within the Results section).

In summary, Figure 9 represents the history of incision within the study area. The T1 level that had formed at an uncertain period during the Mid Quaternary was abandoned during the transition from the peak of the last interglacial (MIS 5e) through towards the end of MIS 5d (by 99 ka) as the river incised. The approximate river corridor width is unknown prior to MIS 5 but is shown to progressively narrow as incision continued throughout MIS 4 and MIS 3. Note that incision was rapid, reaching the deepest point within the bedrock KOM channel sometime prior to 75 ka when aggradation began to fill the KOM channel and river flow would have progressively shifted towards the area of the modern channel. Yet, despite the relatively early incision to form this localized deep and narrow channel, the flood volumes within the main channel were sufficient to laterally plane the T2 strath level that formed from MIS 4 and throughout the first half of MIS 3. The thicknesses of any

aggraded deposits on this strath level are unknown, but were probably thin, as all residual deposits are only a few metres thick at most. A residual alluvial carapace was deposited on the T2 strath during the latter part of MIS 3 into MIS 2. The KOM channel was fully abandoned by 19 ka, shortly after the bed level represented by the higher rock outcrops in the main modern channel was reached around 33 ka. Rapid incision occurred from the MIS 2/MIS 1 transition, leading to preservation of the alluvium on the T2 level by 15 ka, reaching the modern bed level during MIS 1. The T3 level ~ 20 m asl is associated with sub-recent and modern aggradation along the relatively narrow modern river corridor.

5. Conclusions

Three terrace levels occur along the Mekong River in Cambodia, of which the highest, T1 and T2, are the most significant. As well as occurring at different heights above the modern river level, each level can be distinguished by a thin carapace of sands and gravels which differ in character when comparing levels.

The highest T1 level is much degraded, and the age of the initial formation is uncertain, possibly dating from MIS 15, or earlier. Nonetheless, although the timing requires confirmation, the strath terrace level was active when large cobble-sized clasts were deposited near the outer terrace edge, possibly during the peak of glacial sub-stage MIS 5d. The T1 level was abandoned no later than the end of MIS 5d and during the transition to the interglacial substage MIS 5c.

The T2 strath terrace level was initially cut into the bedrock prior to MIS 4 when aggradation occurred on the terrace level. Yet, the thin cover of sediment allowed braiding channels to continue to cut into the bedrock such that the river level (*e.g.*, lower-study-reach; Fig. 3) progressively fell from *c.*, 70 m asl to 41 m asl during the Last Glacial Period. Incision was continuous at the same time as planation of the T2 level occurred, leading to a strath terrace surface that is inclined towards the modern river channel, albeit exhibiting isolated residual hills. The T2 level was abandoned late in MIS 3 when downcutting formed an anastomosed bedrock channel network similar to the modern channel. Notably, incision would have been concentrated within the modern river planform throughout the Last Glacial Maximum (MIS 2). The T3 level is Holocene to modern in age and consists of loamy sand in contrast to the lateritic sand-gravels of the T2 level. Thus, abandonment of the T1

625 and T2 Mekong terrace levels can be associated broadly with transitions from global cool stadials associated 626 with glacial advances in the Himalaya to warmer interstadials when ice retreated. 627 **Author contribution** 628 Paul Carling: Conceptualization; Investigation; Methodology; Formal analysis; Funding acquisition; Project administration; Supervision; Validation; Writing - original draft, review & editing. Luba Meshkova: 629 630 Conceptualization; Investigation; Methodology; Formal analysis; Validation; Visualization; Writing - review & 631 editing. Xuanmei Fan: Funding acquisition; Writing - review & editing. Zhiyong Ding, Ruth Robinson, Tim Kinnaird, Aayush Srivastava: Methodology; Formal analysis; Validation; Writing - review & editing. 632 633 Stephen Darby: Field Investigation; Review & editing. 634 **Declaration of competing interest** 635 The authors declare that they have no known competing financial interests or personal relationships that could have appeared to influence the work reported in this paper. 636 637 **Data availability** All the links and sources of the data used are declared in the article. The majority of the data used to prepare 638 639 this paper are contained within the Tables and within the Supplementary Information. Acknowledgements 640 641 The Mekong River Commission provided the JICA ASTER DEM. Katherine Grant (Australian National 642 University) is thanked for provision of sea level curve data. Ben Savuth (General Department of Mineral 643 Resources, Cambodia) acted as a guide and interpreter. Ross Somerville is thanked for assistance in OSL sample 644 preparation. The commentaries of two anonymous referees were appreciated. 645 **Funding sources** 646 The cosmogenic dating was financially supported by the National Science Fund for Distinguished Young

Scholars of China (Grant 42125702), the Natural Science Foundation Sichuan Province (Grant 22NSFSC0029)

- and the Tencent Foundation through the XPLORER PRIZE (Grant XPLORER-2022-1012), all awarded to
- Xuanmei Fan. P. A. Carling was in receipt of a NERC grant NE/J012440/1 in 2012 in support of fieldwork in
- 650 Cambodia that funded a post-doctoral fellowship for Meshkova. A Leverhulme Trust Emeritus Fellowship
- 651 (EM-2016-010) for Carling underpinned additional work in the region in 2016. Carling collected the rock
- samples for terrestrial cosmogenic dating in 2019 during a fieldwork programme underpinned by a Fostering
- Joint International Research (B) award (# 18KK0092) to Prof. Ryuji Tada (Institute for Geo-Cosmology, Chiba
- 654 Institute of Technology, Japan).

References

655

- Amos, C.B., Burbank, D.W., Nobes, D.C., Read, S.A., 2007. Geomorphic constraints on listric thrust faulting:
- 657 Implications for active deformation in the Mackenzie Basin, South Island, New Zealand. *Journal of Geophysical*
- 658 Research: Solid Earth, 112 (B3). https://doi.org/10.1029/2006JB004291.
- Bao, N. X., Hai, T.Q., 1991. The Indosinian Massif and some problems related to its tectonic evolution in the
- Mesozoic and Cenozoic. Workshop on Geodynamic Evolution of Indochina, Texas A&M University, 15–17
- May 1991, abstracts with programs.
- 662
- Barnett, T.P., Dümenil, L., Schlese, U., Roeckner, E., 1989. The effect of Eurasian snow cover on regional
- and global climate variations. Journal of the Atmospheric Sciences, 46, 661-
- 665 685. https://doi.org/10.1175/1520-0469(1989)046<0661:TEOESC>2.0.CO;2
- Bloom, A. L., Yonekura, N., 1990. Graphic analysis of dislocated Quaternary shorelines. Sea-level change.
- 667 Committee on Global Change, National Research Council, Studies in Geophysics, pp. 104–115. National
- Academy Press, Washington, DC. https://nap.nationalacademies.org/read/1345/chapter/10
- Brookfield, M.E., 1998, The evolution of the great rivers of southern Asia during the India-Asia collision: rivers
- draining southwards. *Geomorphology*, 22, 285-312. https://doi.org/10.1016/S0169-555X(97)00082-2
- 672 Cai, J., Meng, X., Liu, L., Li, G.K., Li, S., Chen, J., Ji, J., 2025. Pleistocene global cooling did not weaken the
- East Asian Summer Monsoon. Journal of Geophysical Research: Atmospheres, 130, e2024JD042746.
- 674 https://doi.org/10.1029/ 2024JD042746
- 675 Cao, L., Shao, L., van Hinsbergen, D.J.J., Jiang, T., Xu, D., 1, Cui, Y., 2023. Provenance and evolution of East
- Asian large rivers recorded in the East and South China Seas: A review. GSA Bulletin, 135, 2723–2752.
- 677 https://doi.org/10.1130/B36559.1
- 678 Carbonnel, J.-P., 1972. Le Quaternaire Cambodgien: Structure et stratigraphie, Paris, France. ORSTOM
- 679 Memoire No. 60, 248pp, horizon.documentation.ird.fr/exl-doc/pleins textes/divers13-11/04538
- 680 Carbonnel, J.-P., Duplaix, S., Selo, M. 1972. La méthode des traces de fission de l'uranium appliquée a la
- 681 géochronologie. Datation du magmatisme recent de l'asie du sud-est. Revue Géographie Physique et de
- 682 Géologie Dynamique, 14, 29-46. https://archive.org/details/sim_revue-de-geologie-dynamique-et-de-
- 683 geographie-physique_1972_14_index

- 684 Carbonnel, J.-P. and Poupeau, G. (1969) Premiers éléments de datations absolues par traces de fission des
- 685 basaltes de l'Indochine méridionale. Earth and Planetary Science Letters, 6, 26-30.
- 686 https://doi.org/10.1016/0012-821X(69)90155-1
- 687 Carling, P.A. 2009. Geomorphology and Sedimentology of the Lower Mekong River. In: Campbell, I.C., Ed.,
- 688 The Mekong Biophysical Environment of an International River Basin, Elsevier, New York, 77-111.
- 689 https://doi.org/10.1016/B978-0-12-374026-7.00005-X/
- 690 Carter, A., Moss, S.J. 1999. Combined detrital-zircon fission-track and U-Pb dating: A new approach to
- 691 understanding hinterland evolution. Geology, 27, 235-238. https://doi.org/10.1130/0091-
- 692 7613(1999)027%3C0235:CDZFTA%3E2.3.CO;2
- 693 Carter, A., Roques, D., Bristow, C.S., 2000. Denudation history of onshore central Vietnam: constraints on the
- 694 Cenozoic evolution of the western margin of the South China Sea. Tectonophysics, 322, 265-277.
- 695 https://doi.org/10.1016/S0040-1951(00)00091-3
- 696 Cheng, H., Li, H., Sha, L., Sinha, A., Shi, Z., Yin, Q., Lu, Z., Zhao, D., Cai, Y, Hu, Y., Hao, Q., Tian, J.,
- Kathayat, G., Dong, X., Zhao, J., Zhang, H. 2022. Milankovitch theory and monsoon. *The Innovation*, 3,
- 698 100338. https://doi.org/10.1016/j.xinn.2022.100338
- 699 Clark, P.U., Shakun, J.D., Baker, P.A., Bartlein, P.J., Brewer, S., Brook, E., Carlson, A.E., Chengh, H.,
- Kaufman, D.S., Liu, Z., Marchitto, T.M., Mix, A.C., Morrill, C., Otto-Bliesner, B.L., Pahnke, K., Russell, J.M.,
- Whitlock, C., Adkins, J.F., Blois, J.L., Clark, J., Colman, S.M., Curry, W.B., Flower, B.P., He, F., Johnson,
- 702 T.C., Lynch-Stieglitz, J., Markgraf, V., McManus, J., Mitrovica, J.X., Moreno, P.I., Williams, J.W., 2012.
- 703 Global climate evolution during the last deglaciation. Proceedings of the National Academy of Sciences, 109,
- 704 E1134-E1142. https://doi.org/10.1073/pnas.1116619109
- 705 Clift, P.D., Layne, G.D., Blusztajn, J., 2004. The erosional record of Tibetan uplift in the East Asian marginal
- seas. In Continent-ocean Interactions within the East Asian Marginal Seas, P.D. Clift, P. Wang, D.E. Hayes, W.
- 707 Kuhnt, American Geophysical Union, Geophysical Monograph 149, 255-282.
- 708 https://doi.org/10.1029/2003EO150005
- 709 Cooper, M., 2000. Mesozoic and Cenozoic thick-skinned deformation in North-east Thailand. Online file
- 710 retrieved from:

- 711 https://webapp1.dlib.indiana.edu/virtual_disk_library/index.cgi/2870166/FID3808/PDF/650.PDF. Last
- 712 accessed 11 March 2024
- 713 Cung, T.C., Dorobek, S., Richter, C., Flower, M., Kikawa, E., Nguyen, Y.T., McCabe, R., 1998.
- 714 Paleomagnetism of Late Neogene Basalts in Vietnam and Thailand: Implications for the Post-Miocene
- 715 Tectonic History of Indochina. 289-299 IN Mantle Dynamics and Plate Interactions in East Asia, M.F.J.
- Flower, S-L Chung, C-H Lo, T-Y Lee (editors), 419 pp, American Geophysical Union, doi:10.1029/GD027
- de Boer, B., Van de Wal Bintanja, R., Lourens, L.J., Tuetter, E., 2010. Cenozoic global ice-volume and
- temperature simulations with 1-D ice-sheet models forced by benthic δ 18O records. Ann. Glaciol. **51**, 23–33.
- 719 doi:10.3189/172756410791392736
- 721 Delgado, J.M., Merz, B., Apel, H., 2012. A climate-flood link for the lower Mekong River. *Hydrol. Earth*
- 722 *Syst. Sci.*, 16, 1533-1541. https://doi.org/10.5194/hess-16-1533-2012
- 723 Egozi, R., Ashmore, P., 2008. Defining and measuring braiding intensity. Earth Surf. Process. Landforms,
- 724 33, 2121–2138. https://doi.org/10.1002/esp.1658

- 726 Finkel, R.C., Owen, L.A., Barnard, P.L., Caffee, M.W., 2003. Beryllium-10 dating of Mount Everest moraines
- indicates a strong monsoon influence and glacial synchroneity throughout the Himalaya. Geology, 6, 561-564. 727
- https://doi.org/10.1130/0091-7613(2003)031%3C0561:BDOMEM%3E2.0.CO;2 728

- 730 Flower, MFJ, Zhang, M, Chen, CY, Tu, K & Xie, G, 1992. Magmatism in the South China Sea Basin. 2.
- Postspreading Quaternary basalts from Hainan Island, South China. Chemical Geology, 97, 65-87. 731
- 732 https://doi.org/10.1016/0009-2541(92)90136-S
- 733 Gao, X., Hao, Q., Wang, L., Song, Y., Ge, J., Wu, H., Xu, B., Han, L., Fu, Y., Wu, X., Deng, C., Guo, Z., 2024.
- Changes in monsoon precipitation in East Asia under 2°C interglacial warming. Science Advances, 10. 734
- 735 https://doi.org/10.1126/sciadv.adm7694
- 736 Germanoski, D., Schumm, S.A., 1993. Changes in braided river morphology resulting from aggradation and
- degradation. Journal of Geology, 101, 451–466. https://www.jstor.org/stable/30068799 737

738

- 739 Grant, K.M., Rohling, E.J., Bronk Ramsey, C., Cheng, H., Edwards, R.L., Florindo, F., Heslop, D., Marra, F.,
- 740 Roberts, A.P. Tamisiea, M.E., Williams, F., 2014. Sea-level variability over five glacial cycles. *Nature*
- 741 Communications, 5:5076, https://doi: 10.1038/ncomms6076

742

743 Hancock, G.S., Anderson, R.S., 2002. Numerical modelling of fluvial strath-terrace formation in response to

744 oscillating climate. Geological Society of America Bulletin, 114, 1131-1142. 745

746

- Hansen, J., Sato, M., Russell, G., Kharecha, P., 2013. Climate sensitivity, sea level and atmospheric carbon
- 747 dioxide. Phil Trans R Soc A, 371: 20120294. http://dx.doi.org/10.1098/rsta.2012.0294

748

- 749 Hanebuth, T.J.J., Stattegger, K., Bojanowski, A., 2009. Termination of the Last Glacial Maximum sea-level
- Global and Planetary 750 Sunda-Shelf data revisited. Change.
- 751 https://doi.org/10.1016/j.gloplacha.2008.03.011
- 752 Hanebuth, T.J.J., Stattegger, K., Grootes, P.M., 2000. Rapid flooding of the Sunda Shelf: A Late-Glacial sea-
- 753 level record. Science, 288, 1033-1035. doi: 10.1126/science.288.5468.1033

754

- 755 Hanebuth, T.J.J., Voris, H.K., Yokoyama, Y., Saito, Y., Okuno, J., 2011. Formation and fate of sedimentary
- depocentres on Southeast Asia's Sunda Shelf over the past sea-level cycle and biogeographic implications. 756
- Earth-Science Reviews, 104, 92-110. https://doi.org/10.1016/j.earscirev.2010.09.006 757

758

- 759 Hennig, J., Breitfeld, H.T., Gough, A., Hall, R., Long, T.V., Kim, V.M., and Quang, S.D., 2018, U-Pb zircon
- 760 ages and provenance of Upper Cenozoic sediments from the Da Lat zone, SE Vietnam: Implications for an
- 761 intraMiocene unconformity and paleo-drainage of the proto-Mekong River. Journal of Sedimentary Research,
- 762 88, 495–515, https://doi.org/10.2110/jsr.2018.26

763

- 764 Hoang, N., Flower, M., 1998. Petrogenesis of Cenozoic basalts from Vietnam: implications for origins of a
- 765 diffuse igneous province. J. Petrology, 39, 369-395. https://doi.org/10.1093/petroj/39.3.369
- 766 Hobart, B., Lisiecki, L.E., Rand, D., Lee, T., Lawrence, C.E., 2023. Late Pleistocene 100-kyr glacial cycles
- 717-722. 767 precession forcing of summer insolation. Nature Geoscience, 16,
- 768 https://doi.org/10.1038/s41561-023-01235-x
- 769 Hurst, M.D., Rood, D.H., Ellis, M.A., 2016. Controls on the distribution of cosmogenic 10Be across shore
- 770 platforms. Earth Surf. Dynam. Discuss., doi:10.5194/esurf-2016-42

- 772 Inoue, T., Izumi, N., Shimizu, Y., Parker, G., 2014. Interaction among alluvial cover, bed roughness, and
- 773 incision rate in purely bedrock and alluvial-bedrock channel. Journal of Geophysical Research: Earth
- 774 Surface, 119: F03018. https://doi.org/10.1002/2014JF003133

- Imbrie, J., Boyle, E.A., Clemens, S.C., Duffy, A., Howard, W.R., Kukle, G., Kutzbach, J., Martinson, D.G.,
- McIntyre, A., Mix, A.C., Molfino, B., Morley, J.J., Peterson, L.C., Pisias, N.G., Prell, W.I., Raymo, M.E.,
- 578 Shackleton, N.J., Toggweiler, J.R., 1992. On the structure and origin of major glaciation cycles 1. Linear
- responses to Milankovitch forcing. *Palaeoceanography*, 7, 701-738. https://doi.org/10.1029/92PA02253

780

- JICA (Japanese International Cooperation Agency), 2003. Cambodia Reconnaissance Survey Digital Data,
- 782 Ministry of Public Works and Transportation (MPWT), Kingdom of Cambodia, [digital data set].
- 783 https://www.jica.go.jp/

784

- Jones, R.S., Small, D., Cahill, N., Bentley, M.J., Whitehouse, P.L., 2019. iceTEA: Tools for plotting and
- analysing cosmogenic-nuclide surface-exposure data from former ice margins. *Quaternary Geochronology*,
 - 51, 72-86. https://doi.org/10.1016/j.quageo.2019.01.001

787 788

- Kenworthy, M.K., Rittenour, T.M., Pierce, J.L., Sutfin, N.A., Sharp, W.D., 2014, Luminescence dating
- 790 without sand lenses: An application to coarse-grained alluvial fan deposits of the Lost River Range, Idaho,
- 791 USA. Quaternary Geochronology, 23, 9-25. http://dx.doi.org/10.1016/j.quageo.2014.03.004

792

- Lai, Z., Zhao, Q., Yan, Y., Li, D., Liu, B., Liu, K., Huang, B., Zhang, P., 2023. Mesozoic evolution of large-
- scale drainage systems in Indochina Block: evidence from paleomagnetic and U-Pb geochronological
- 795 constraints. Journal of the Geological Society, VOL and pp, doi: https://doi.org/10.1144/jgs2023-084
- Lal, D., 1991. Cosmic-ray labeling of erosion surfaces: in situ nuclide production rates and erosion models.
- 797 Earth Planet. Sc. Lett., 104, 424–439. https://doi.org/10.1016/0012-821X(91)90220-C

798

- The Tee, G.H., Lee, K., Watkins, J.S., 2001. Geological evolution of the Cu Long and Nam Con Son basins, offshore
- southern Vietnam, South China Sea. AAPG Bulletin, 85, 1055-1082. https://doi.org/10.1306/8626CA69-173B-
- 801 11D7-8645000102C1865D
- Lee, G.H., Watkins, J.S., 1998. Seismic sequence stratigraphy and hydrocarbon potential of the Phu Khanh
- 803 Basin offshore central Vietnam, South China Sea. AAPG Bulletin, 82, 1711-1735.
- 804 https://doi.org/10.1306/1D9BCB83-172D-11D7-8645000102C1865D
- 805 Leuschner, D.C., Sirocko, F., 2003. Orbital insolation forcing of the Indian Monsoon a motor for global
- 806 climate changes? Palaeogeography, Palaeoclimatology, Palaeoecology, 197, 83-95.
- 807 https://doi.org/10.1016/S0031-0182(03)00387-0

808

- Li, W., Colombera, L., Yue, D., Mountney, N.P., 2023. Controls on the morphology of braided rivers and braid
- 810 bars: An empirical characterization of numerical models. Sedimentology, 70, 259-279.
- 811 https://doi.org/10.1111/sed.13040

812

- Lifton, N., Beel, C., Hättestrand, C., Kassab, C., Rogozhina, I., Heermance, R., Oskin, M., Burbank, D.,
- Blomdin, R., Gribenski, N., Caffee, M., Goehring, B. M., Heyman, J., Ivanov, M., Li, Y., Li, Y., Petrakov, D.,
- Usubaliev, R., Codilean, A. T., Chen, Y., Harbor, J., and Stroeven, A. P., 2014. Constraints on the late
- Quaternary glacial history of the Inylchek and Sary-Dzaz valleys from in situ cosmogenic 10Be and 26Al,
- eastern Kyrgyz Tian Shan. Quaternary Science Reviews, 101, 77-90, 10.1016/j.quascirev.2014.06.032.
- 818 https://doi.org/10.1016/j.quascirev.2014.06.032

819

- 820 Liu, Z., Huang, W., Li, J., Wang, P., Wang, R., Yu, K., Zhao, J., 2009. Sedimentology. 171–296 In:
- Wang, P., Li, Q. (Eds.), The South China Sea: Paleoceanography and Sedimentology. Springer, Dordrecht, the
- 822 Netherlands.

- 824 Löffler, E., Thompson, W.P., Liengsakul, M., 1984. Quaternary geomorphological development of the Lower
- 825 Mun River Basin, North East Thailand. *Catena*, 11, 321-330. https://doi.org/10.1016/S0341-8162(84)80030-2
- Matthews, SJ, Fraser, AJ, Lowe, S, Todd, SP & Peel FJ, 1997. Structure, stratigraphy, and petroleum geology
- of the SE Nam Con Son Basin, offshore Vietnam. In AJ Fraser, SJ Matthews and RW Murphy, eds, Petroleum
- 828 Geology of Southeast Asia: Geological Society Special Publication, 126, 89-106.
- https://www.lyellcollection.org/doi/abs/10.1144/GSL.SP.1997.126.01.07
- 830 Meshkova, L.V. Carling, P.A. 2012. The geomorphological characteristics of the Mekong River in northern
- 831 Cambodia: A mixed bedrock–alluvial multi-channel network. *Geomorphology*, 147-148, 2-17.
- 832 https://doi.org/10.1016/j.geomorph.2011.06.041
- 833
- Meshkova, L.V., Carling, P.A., Buffin-Bélanger, T., 2013. Nomenclature, complexity, semi-alluvial channels
- and sediment-flux-driven bedrock erosion. Gravel-Bed Rivers: Processes, Tools, Environments, Church M,
- 836 Biron PM, Roy AG (eds). John Wiley and Sons Ltd, https://doi.org/10.1002/9781119952497.ch31
- 837

- Métivier, F., Gaudemer, Y., Tapponnier, P., Klein, M., 1999. Mass accumulation rates in Asia during the
- 839 Cenozoic. *Geophys. J. Int.*, 137, 280–318. https://doi.org/10.1046/j.1365-246X.1999.00802.x
- Murari, M.K., Owen, L.A., Dortch, J.M., Caffee, M.W., Dietsch, C., Fuchs, M., Haneberg, W.C., Sharma,
- M.C., Townsend-Small, A., 2014. Timing and climatic drivers for glaciation across monsoon-influenced
- regions of the Himalayan-Tibetan orogen. Quat. Sci. Rev. 88, 159e182.
- 844 http://dx.doi.org/10.1016/j.quascirev.2014.01.013
- 845

- 846 Murray, A.S., Wintle, A.G., 2000. Luminescence dating of quartz using an improved single-aliquot
- regenerative-dose protocol. *Radiat. Meas.* 32, 57–73. https://doi. org/10.1016/S1350-4487(99)00253-X
- 849 Murray, A.S., Wintle, A.G., 2003. The single aliquot regenerative dose protocol: potential for improvements
- 850 in reliability. *Radiat. Meas.* 37, 377–381. https://doi.org/ 10.1016/S1350-4487(03)00053-2.
- Murray, M.R., Dorobek, S.L., 2004. Sediment supply, tectonic subsidence, and basin-filling patterns across
- the Southwestern South China Sea during Pliocene to Recent time. Geophysical Monograph Series, 149, 235-
- 853 254.
- NGRIP Members, (2004). High-resolution record of Northern Hemisphere climate extending into the last
- 855 interglacial period. *Nature*, 431, 147-151. www.nature.com/nature
- 856
- 857 Nakada, M., Lambeck, K., 1989. Late Pleistocene and Holocene sea level change in the Australian region and
- mantle rheology. *Geophysical Journal International*, 96, 497–517. https://doi.org/10.1111/j.1365-
- 859 246X.1989.tb06010.x
- 860
- Nie, J., Ruetenik, G., Gallagher, K., Hoke, G., Garzione, C. N., Wang, W., Stockli, D., Hu, X., Wang, Z.,
- Wang, Y., Stevens, T., DanišÍk, M., & Liu, S., 2018. Rapid incision of the Mekong River in the middle
- Miocene linked to monsoonal precipitation. *Nature Geoscience*, 11, 944-948. https://doi.org/10.1038/s41561-
- 864 018-0244-z
- Owen, L.A., 2009. Latest Pleistocene and Holocene glacier fluctuations in the Himalaya and Tibet.
- 866 *Quaternary Science Reviews*, 28, 2150-2164. https://doi.org/10.1016/j.quascirev.2008.10.020
- 867 Owen, L.A., 2010. Landscape development of the Himalayan-Tibetan orogen: a review. Special
- Publication of the Geological Society of London, 338, 389-407. https://doi.org/10.1144/SP338.18
- Owen, L.A., Caffee, M.W., Finkel, R.C. and Seong, B.Y., 2008. Quaternary glaciations of the Himalayan-
- Tibetan orogen. Journal of Quaternary Science. 23, 513-532. https://doi.org/10.1002/jqs.1203

- Owen, L.A., Dortch, J.M., 2014. Nature and timing of Quaternary glaciation in the Himalayan-Tibetan
- orogen. Quaternary Science Reviews, 88, 14-54. https://doi.org/10.1016/j.quascirev.2013.11.016
- Owen, L.A., Finkel, R.C., Caffee, M.W., 2002. A note on the extent of glaciation throughout the Himalaya
- during the global Last Glacial Maximum. *Quaternary Science Reviews*, 21, 147-157.
- 875 https://doi.org/10.1016/S0277-3791(01)00104-4
- Owen, L.A., Robinson, R., Benn, D.I., Finkel, R.C., Davis, N.K., Yi, C., Putkonen, J., Li, D. and Murray,
- 877 A.S., 2009. Quaternary glaciation of Mount Everest. *Quaternary Science Reviews*, 28, 1412-1433.
- 878 https://doi.org/10.1016/j.quascirev.2009.02.010
- Pan, B., Burbank, D., Wang, Y., Wu, G., Li, J., Guan, Q., 2003. A 900 ky record of strath terrace formation
- during glacial-interglacial transitions in Northwest China. *Geology*, 31, 957–960.
- 881 https://doi.org/10.1130/G19685.1
- 882
- Peterse, F., Prins, M. A., Beets, C.J., Troelstra, S.R., Zheng, H., Gu, Z., Schouten, S., Sinninghe Dansté, J.S.,
- 2011. Decoupling warming and monsoon precipitation in East Asia over the last deglaciation. *Earth and*
- 885 *Planetary Science Letters*, 301, 256-264. http://dx.doi.org/10.1016/j.epsl.2010.11.010
- 886
- Pratte, S., Bao, K., Li, C., Zhang, W., Le Roux, G., Li, G., De Vleeschouwer, F., 2024. East Asian monsoon
- and westerly jet driven changes in climate and surface conditions in the NE drylands of China since the Late
- 889 Pleistocene. Quaternary Science Reviews, 331, 108637. https://doi.org/10.1016/j.quascirev.2024.108637
- 890
- Prell, W.L., Kutzbach, J.E., 1992. Sensitivity of the Indian monsoon to forcing parameters and implications
- for its evolution parameters and implications for its evolution. *Nature*, 360, 647-652.
- 893
- Racey, A., 2009. Mesozoic red bed sequences from SE Asia and the significance of the Khorat Group of NE
- Thailand. pp 41-67 In: E. Buffetaut, G. Cuny, J. Le Loeuff & V Suteethorn (eds), Late Palaeozoic and
- Mesozoic Continental Ecosystems in SE Asia. The Geological Society, London, Special Publications, 315,
- 897 41–67, The Geological Society of London. doi: 10.1144/SP315.5 0305-8719/09
- 898
- 899 Rangin, C., Huchon, P., Le Pichon, X., Bellon, H., Lepvrier, C., Roques, D., Nguyen, D.H., Phan, V.Q., 1995.
- 900 Cenozoic deformation of central and southern Vietnam. Tectonophysics, 251, 179-196.
- 901 https://doi.org/10.1016/0040-1951(95)00006-2
- 902 Rhodes, E., 2011. Optically stimulated luminescence dating of sediments over the past 200,000 years. *Annual*
- 903 Review of Earth and Planetary Sciences, 39, 461-488.
- 904 https://www.annualreviews.org/doi/pdf/10.1146/annurev-earth-040610-133425
- Rohling, E.J., Grant, K., Bolshaw, M., Roberts, A.P., Siddall, M., Hemleben, C., Kucera, M., 2009. Antarctic
- temperature and global sea level closely coupled over the past five glacial cycles. *Nat. Geosci.* 2, 500–504.
- 907 doi:10.1038/ngeo557

- 909 Rupper, S., Roe, G., Gillespie, A., 2009. Spatial patterns of Holocene glacier advance and retreat in Central
- 910 Asia. *Quaternary Research*, 72, 337-346. https://doi.org/10.1016/j.ygres.2009.03.007
- 911 Sasada, M., Ratanasthien, B., Soponpongpipat, P., 1987. New K-Ar ages from the Lampang basalt, northern
- 912 Thailand. Bulletin of the Geological Survey of Japan, 38, 13-20. https://www.gsi.jp/en/publications/bull-
- 913 gsj/index.html
- 914 Saurin, E., 1935. Etude geologique sur l'Indochine du Sud-Est (Sud Annam, Cochinchine, Cambodge oriental),
- 915 Bull. Serv. Geol Indochine. XXII. 420. https://documentation-
- 916 beauvais.unilasalle.fr/index.php?lvl=notivr_display&id=9559

- 917 Saurin, E., 1966. Le Paléolithique du Cambodge Oriental, Asian Perspectives, 9, 96-109.
- 918 https://www.jstor.org/stable/42928961
- 919 Saurin E, 1967. La neotectonique de l'Indochine. Rev Geol Dynam Geog Phys, 9: 143-152.
- 920 Sladen, C. P. 1994. Key elements during the search for hydrocarbons in lake basins. In: E. Gierlowskikordesh,
- 921 E. & K. Kelts (eds), Global Record of Lacustrine Basins. Cambridge University Press, Vol. 1, 3-17. 978-0-521-
- 922 03168-4
- 923 Sladen, C.P., 2012. Lake Systems, In: D.G. Roberts and A.W. Bally (Eds.) Regional Geology and Tectonics:
- 924 Principles of Geological Analysis, 406-450, Elsevier, https://doi.org/10.1016/B978-0-444-53042-4.00015-7
- 925 Sieh, K., Herrin, J., Jicha, B., Schonwalder, D., 2020. Australasian impact crater buried under the Bolaven
- 926 volcanic field, Southern Laos. *Proceedings of the National Academy of Sciences*, 117, 201904368. Doi:
- 927 10.1073/pnas.1904368116
- 928
- 929 Sieh, K., Angel, D.S., Herrin, J., Jicha, B., Singer, B., Sihavong, V., Wiwegin, W., Wong, N., Quah, J.Y.
- 930 (2023) Proximal ejecta of the Bolaven extraterrestrial impact, southern Laos. *Proceedings of the National*
- 931 Academy of Science, 120, https://www.pnas.org/doi/epdf/10.1073/pnas.2310351120

- 933 Simons, W. J. F., Socquet, A., Vigny, C., Ambrosius, B.A.C., Haji Abu, S., Promthong, C., Subarya, C.,
- 934 Sarsito, D.A., Matheussen, S., Morgan, P., Spakman, W., 2007. A decade of GPS in Southeast Asia:
- 935 Resolving Sundaland motion and boundaries. J. Geophys. Res., 112, B06420, doi:10.1029/2005JB003868.

936

- 937 Slingerland, R., Smith, N.D., 2004. River avulsions and their deposits. *Annual Review of Earth and Planetary*
- 938 Sciences, 32, 257-285. https://doi.org/10.1146/annurev.earth.32.101802.120201

939

- 940 Smith, L. C., Isacks, B.L., Bloom, A.L., Murray, A.B., 1996. Estimation of discharge from three braided
- 941 rivers using synthetic aperture radar (SAR) satellite imagery: potential application to ungaged basins. *Water*
- 942 Resources Research, 32, 2021–2037. https://doi.org/10.1029/96WR00752

943

- 944 SNMGP (Service National Des Mines, de la Géologique et du Pétrole), 1973. Carte Géologique de
- P45 Reconnaissance. République Khmére. Scale 1:200,000, Paris. https://www.sudoc.fr/036142182

946

- 947 Stapledon, D.H., Wood, C.C., McCahon, B.K., Harrison, J., 1962. Geological Investigations Sambor Dam
- 948 site, Cambodia. Geological Report, Colombo Plan, Snowy Mountains Hydro-electric Authority, Cooma,
- Australia, Vol. 1, p. 61. Plus, drill logs and drawings. https://nla.gov.au/nla.obj-741048037 (accessed October
- 950 2023)

951

- 952 Steinhouer, D.W., Qiang, J., McCabe, P.J.M., Ryder, R.T., 1997. Maps showing geology, oil and gas field,
- 953 and geological provinces of the Asia Pacific region, U.S. Geological Survey Open-File Report 97-470F.
- 954 https://pubs.usgs.gov/publication/ofr97470F

955

- 956 Takaya, Y., 1967. Observations on some Pleistocene outcrops in Cambodia. *The Southeast Asian Studies*
- 957 'Kyoto University', V, 122–137. https://repository.kulib.kyoto-
- 958 u.ac.jp/dspace/bitstream/2433/55421/1/KJ00000133426.pdf

959

- 960 Tjallingii, R., Stattegger, K., Stocchi, P., Saito, Y., Wetzel, A., 2014. Rapid flooding of the southern Vietnam
- shelf during the early to mid-Holocene. *Journal Of Quaternary Science*, 29, 581–588. DOI: 10.1002/jqs.2731.

- Turowski, J.M., Rickenmann D., 2008. Tools and cover effects in bedload transport observations in the
- Pitzbach, Austria. Earth Surface Processes and Landforms, 34: 26–37. https://doi.org/10.1002/esp.1686

- 966 UN (United Nations), 1993. Atlas of Mineral Resources of the ESCAP Region, Explanatory Brochure, vol 10,
- 967 Cambodia, New York, 87pp. https://repository.unescap.org/

968

- 969 Vozenin-Serra, C., Privé-Gill, C. 1991. Les terrasses Iluviales pléistocenes du Mékong (Cambodge). II Bois
- 970 silicifiés homoxylés récoltés entre Stung-Treng et Snoul. Review of Palaeobotony and Palynology, 68, 87-
- 971 117. (in French)

972

- Wang, L., Shen, L., Liu, C. and Ding, L. 2020a. Evolution of the paleo-Mekong River in the Early
- 974 Cretaceous: Insights from the provenance of sandstones in the Vientiane Basin, central Laos.
- 975 Palaeogeography, Palaeoclimatology, Palaeoecology, 545, 109651,
- 976 https://doi.org/https://doi.org/10.1016/j.palaeo.2020.109651

- 978 Wongsomsak, S., 1992. Preliminary investigation on Mekong terraces in Nakhon Phanom Province:
- 979 Distribution, characteristics, age, and implications. Proceedings of a National Conference on Geologic
- 980 Resources of Thailand: Potential for future Development. Department of Mineral Resources, Bangkok, 326-
- 981 331.
- 282 Zhou, Y., Han, J., Shen, Q., Xu, Y., Tao, Y., Lin, P., Lai, Y., Wang, Y., Lai, Z., 2024. Orbital global change
- 983 drove fluvial aggradation and incision in Tibetan upper Mekong river: Chronological perspectives. *Quaternary*
- 984 *Geochronology*, 82, 101546. https://doi.org/10.1016/j.quageo.2024.101546
- Zondervan, J.R., Stokes, M., Telfer, M.W., Boulton, S.J., Mather, A.E., Buylaert, J.-P., Jain, M., Murray, A.S.,
- Belfoul, M.A., 2022. Constraining a model of punctuated river incision for Quaternary strath terrace formation.
- 987 *Geomorphology*, 414, 108396. https://doi.org/10.1016/j.geomorph.2022.108396.

Table 1:10Be apparent exposure ages calculated using CRONUS online calculator.

Sample	Quartz	9Be	10Be/9Be	Northing	Easting (°)	¹⁰ Be concentration	Alt.of	St			Lm			LSDn		
		carrier		(°)			sample									
ID ^a	(g)	(g)	(10 ⁻¹⁵)			(10 ³ atoms/g)		Age	Internal	External	Age	Internal	External	Age	Internal	External
		107					(m)		error	error		error	error		error	error
								(years)	(years)	(years)	(years)	(years)	(years)	(years)	(years)	
																(years)
1F	40.1793	0.2737	191±13.52	13.08070	106.05460	81125.05±5817.56	28	30777	2224	3309	27224	1966	2844	33033	2388	3093
LZ-blank1		0.2781	0.546			9495.24±0										
2F	40.2112	0.2757	336±22.81	13.00727	106.15025	143784.73±9887.14	68	53511	3729	5680	45587	3171	4692	57735	4028	5307
3F	40.1412	0.2759	597±25.77	13.177871	106.172055	256319.87±11367.59	80	95756	4350	8886	84296	3818	7502	99420	4521	7524
LZ-blank2		0.2772	0.635			11043±0										

^aSandstone lithology

Table 2: Summary of OSL dates and ¹⁴C date.

Location	Sample # in Fig. 3	Terrace #	Height above river ¹ (m)	Altitude of surface (m)	Depth of sample (m)	Northing (°)	Easting (°)	OSL date/Radiocarbon ² (ka)	Relative position of sample	Material
Koh Preah	01	T2	13	55	1.85	13.293283	105.973817	70.65 ± 5.13	Outer margin T2	Basal sand
Koh Preah	02	T2	14	55	0.80	13.293283	105.973817	38.66 ± 2.40	Outer margin T2	Sand in near basal gravel
Koh Preah	О3	T2	14.5	55	0.55	13.285733	105.974417	14.72 ± 0.95	Outer margin T2	Sand just above basal gravel
Srê Sbov	O4	T2	45	72	1.10	12.878889	106.196167	21.29 ± 1.76	Inner margin T2	Clay-rich sand below basal gravel
Srê Sbov	O5	T2	45.3	72	0.70	12.878889	106.196167	0.08 ± 0.01	Inner margin T2	Sand
Koh Knaja	O6	T2	13.8	48	1.2	13.112167	106.069944	2.56 ± 0.18	Outer margin T2	Silt just above bedrock
Koh Knaja	07	T2	14	48	1.0	13.112167	106.069944	0.32 ± 0.04	Outer margin T2	Sand just above gravel layer
Koh Knaja	08	T2	13.9	48	1.1	13.112167	106.069944	0.01 ± 0.01	Outer margin T2	Silt and granules
Koh Knaja	09	T2	14	48	1.0	13.112167	106.069944	0.23 ± 0.04	Outer margin T2	Sand matrix from gravel layer
Koh Knaja	O10	T2	14.1	48	0.9	13.112167	106.069944	2.93 ± 0.27	Outer margin T2	Sand
Kbal Damrei	011	T2	75	97	1.95	12.898967	106.222817	13.86 ± 1.44	Outer margin T1	Sand matrix in gravel
Prek Chamlak	¹⁴ C	Т3	10	20	6	12.357869	106.061169	0.450 ± 0.050	Outer margin T3	² Wood in basal clay
Palaeo- channel	Mek 5	Borehole KOM		25	4.12 to 4.16	12.610194	105.989444	19.43 ± 1.96 ka		Silt
Palaeo- channel	Mek 4	Borehole KOM		25	4.65 to 4.69	12.610194	105.989444	43.21 ± 3.11 ka		Sand
Palaeo- channel	Mek 3	Borehole KOM		25	5.12 to 5.18	12.610194	105.989444	39.20 ± 4.45 ka		Sand
Palaeo- channel	Mek 2	Borehole KOM		25	5.47 to 5.52	12.610194	105.989444	75.43 ± 5.72 ka		Sand & Clay

¹ Approx. heigh of sample above modern low flow water level; ² Radio-carbon dating sample for Prek Chamlak